THESIS FOR THE DEGREE OF LICENTIATE OF ENGINEERING

in

Thermo and Fluid Dynamics

Numerical Investigations of Incompressible Turbomachinery Applications using OpenFOAM

by

OLIVIER PETIT

Department of Applied Mechanics
CHALMERS UNIVERSITY OF TECHNOLOGY
Göteborg, Sweden, 2010

Numerical Investigations of Incompressible Turbomachinery Applications using OpenFOAM
OLIVIER PETIT

THESIS FOR LICENTIATE OF ENGINEERING no. 2010:02
ISSN 1652-8565

Department of Applied Mechanics
Chalmers University of Technology
SE-412 96 Göteborg
Sweden
Telephone +46-(0)31-7721000

This document was typeset using LaTeX

Printed at Chalmers Reproservice
Göteborg, Sweden, 2010

Numerical Investigations of Incompressible Turbomachinery Applications using OpenFOAM

by

Olivier Petit

Division of Fluid Dynamics
Department of Applied Mechanics
Chalmers University of Technology
SE-412 96 Göteborg, Sweden
olivierp@chalmers.se

Abstract

Swirling flow and unsteady phenomena are common in technical applications, such as turbines, pumps and compressors. The objective of this work is to get a good understanding of the turbulent flow features inside such applications, and to validate the computational techniques used for such applications.

Because of the complexity of the turbulent flow, approximations are made when solving the flow equations in the computational domain. Depending on the level of the approximations, the level of accuracy and detail in the predicted flow will vary. To validate the assumptions used in the simulations and to get a good prediction of the flow, the computational technique as well as the CFD code must thus be validated against detailed measurements. The present work aims at getting a good understanding of the turbulent flow in the U9 Kaplan turbine model, using the OpenFOAM CFD code. Detailed measurements are used to validate the computed turbulent flow features.

Two methods are used in this present work to predict the interaction between rotating and stationary parts of the machines. The steady-state method coupled with the frozen rotor approach solves the time-averaged Reynolds Averaged Navier Stokes equations, while the unsteady method with the sliding grid approach solves the same equations taking the time dimension into account. To validate the two different computational techniques, comparisons between computational results and detailed measurements for two different case studies are performed: the ERCOFTAC centrifugal pump, and a swirl generator test rig. Good agreement is found between numerical and experimental results.

Acknowledgements

This work was conducted at the Division of Fluid Dynamics, Department of Applied Mechanics, Chalmers University of Technology.

The research presented in this thesis was carried out as a part of the Swedish Hydropower Centre (SVC). SVC was established by the Swedish Energy Agency, Elforsk, Swedish companies related to water power[1], and Svenska Kraftnät together with Luleå University of Technology, The Royal Institute of Technology, Chalmers University of Technology and Uppsala University. Their financial support is gratefully acknowledged.

I also would like to express my thanks to my colleagues that shared their experimental work with me in order to realize the validations: Professor Ubaldi and her team for the measurements on the ERCOFTAC centrifugal pump, Professor Romeo F.Susan-Resiga, Sebastian Muntean, Alin Bosioc and their team for the measurements on the swirling flow test rig, and Berhanu Mulu for the detailed database on the U9 Kaplan turbine model.

I would like to acknowledge the Swedish National Infrastructure for Computing (SNIC) and Chalmers Centre for Computational Science and Engineering (C^3SE) for providing computational resources.

I would like to thank some of my colleagues on the other side of the Atlantic ocean: Maryse Page, Martin Beaudoin, Anne Marie Giroux and all her team, who welcomed me for six months in Québec, and made me feel at home. My sincere gratitude for the friendship and knowledge shared along the way, merci beaucoup!! I would like also to ackowledge Thi Vu and its team at Andritz, Canada, for the help and collaboration for this project.

Finally I would like to thank my supervisor, Håkan Nilsson. His patience and knowledge made this work enjoyable and allowed me to progress quickly. I would like to acknowledge as well my colleagues and employees at the Division of Fluid Dynamics for creating a stimulating and fun working atmosphere.

[1]Andritz Hydro, E.ON Vattenkraft Sverige, Fortum Generation, Holmen Energi, Jämtkraft, Karlstads Energi, Linde Energi, Mälarenergi, Skellefteå Kraft, Sollefteå forsens, Statkraft Sverige, Statoil Lubricants, Sweco Infrastructure, Sweco Energuide, SveMin, Umeå Energi, Vattenfall Research and Development, Vattenfall Vattenkraft, VG Power and WSP.

Contents

Introduction

Most of the Earth's energy comes from the sun. Some of this energy is stored in the depth of the planet as fossil fuels (oil, coal, etc.). Some of it can be harvested at once, such as the energy contained in the wind, the sun's rays or the flow of water. Already during the Roman periods, the potential and kinetic energy of the wind or the flow of water was transformed into useful mechanical energy.

It is only in the end of the 19^{th} century that the hydro energy started to be used to generate electricity. Due to the many advantages of hydro electricity, hydro power stations soon started springing up. Nowadays, due to climate change issues related to the greenhouse gas effect, coupled with the prospect of lacking fossil fuels in the coming decades, hydro power is a very appealing source of energy and is widely used. The impact on the environment is minimal. While in production, a hydraulic turbine does not produce emission, and leaves behind no waste. It is a 100% renewable energy source. Hydro power is providing around 17.5% of the world's electricity, accounting for almost 85% of electricity from renewable sources [1].

An overview of a hydro power plant is shown in Fig.1. When water is stored in a dam, its kinetic energy is negligible compared to its potential energy. The available potential energy of the water is proportional to the difference in the water surface level in the dam, and that of the reservoir to which the water is flowing. This height is called the static head. The potential energy is converted into mechanical energy due to the flow out of the dam, through a water turbine. The power of a hydro power station is thus directly related to the static head and to the flow rate of the water in the turbine. Depending on those two parameters, different types of turbines can be used. The two most common types of turbines are the Kaplan turbine (Fig.2(a)), which commonly operates in a low head range (10-60 m), and the Francis turbine (Fig.2(b)) which head can vary between 10 to several hundred meters. However, Francis turbines are sometimes used for low head range as well. Sweden has many small hydro power stations with such examples.

A water turbine is composed of four main parts:

- The spiral casing. The purpose of the spiral casing is to distribute the water flow evenly over the whole runner inlet, as well as to create a swirl. The creation of the swirl is in fact a conversion of some of the static energy to kinetic energy.

- The guide vanes. The function of the guide vanes is to regulate the

water flow. Through the guide vanes, it is also possible to control accurately the swirl that goes into the runner.

- The runner. This is the part where most of the total energy is converted into mechanical energy. Almost all the swirl entering the runner is removed as it flows through the runner.
- The draft tube ("axial diffusor" in Fig.2(a) and Fig.2(b)). Located downstream of the runner, its purpose is to reduce the velocity of the flow with as minimum energy loss as possible. The remaining kinetic energy of the flow is thus converted back to potential energy.

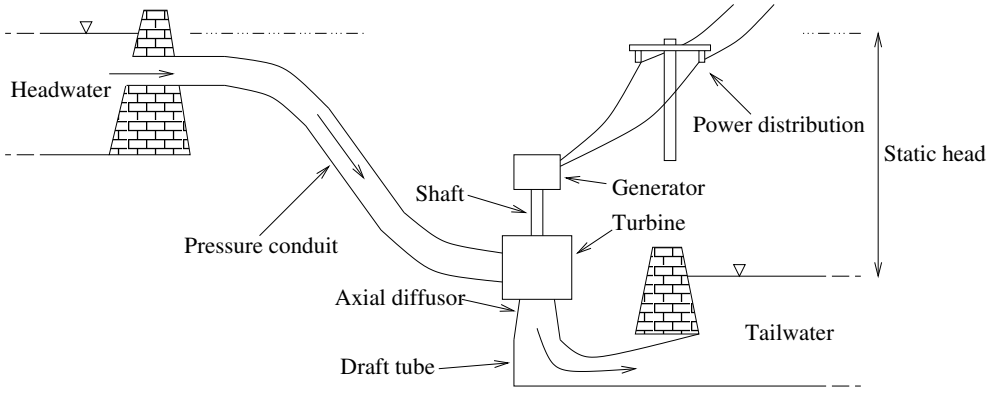

Figure 1: Overview of a hydraulic power plant.

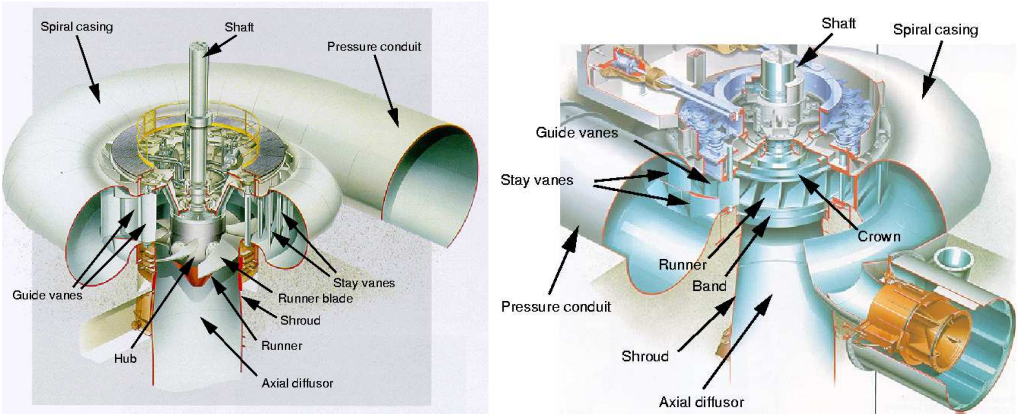

(a) Kaplan turbine

(b) Francis turbine

Figure 2: Overview of the two main turbine designs.

The life of a hydraulic power plant is in general longer than any other power plants. Some power plants have run more than 100 years. Though the dam itself stays unchanged, the water turbines get damaged, due for example to cavitation problems or vibration in the shaft between the turbine and the generator. Due to those diverse issues, some turbine parts need to be

replaced. With time comes new technology, and new designs. It is the case for the Porjus hydraulic power plant, located in the north of Sweden. Active since 1915, one of its units (turbine and generator), called U9 was replaced during the last decade. The main focus of the new U9 unit is to allow research on a real scale turbine, rather than production of electric power [2]. It is difficult to find detailed measurements of the flow in water turbines. Very few detailed measurements are made since it is overall quantities such as efficiency that are important at design phase. Furthermore, the few existing databases are often kept confidential, and are usually realized on a scaled model. To create a detailed database on a real scale turbine requires the possibility to start and stop the turbine often, thus stopping the electricity production and loosing money. Therefore measurements on real scale turbines are rarely performed. The U9 turbine presents a unique way to do measurements on a real scale water turbine, and to validate computational techniques on a complex geometry. In this work, however, the computed flow is compared to detailed measurements realized on a 1:3.1 scale model of the U9 Kaplan turbine. The U9 model is mounted on a test rig located in Älvkarleby, at VattenFall Research and Development (VRD).

CFD in water turbines

Computational fluid dynamics (CFD) is a widely used tool for simulation of fluid flow. With a broad diversity of numerical models, CFD brings the possibility to approximate the flow features differently. For example, the Euler method neglects the effects of viscosity and turbulence. Using a large amount of approximations allows to compute the problem faster, but does not resolve all the details of the flow. If too large approximations are made, some of the important features of the flow will be unpredicted, thus not reflecting the reality of the flow. Nowadays, the effect of the viscosity of the fluid is included, rather than solving equations for inviscid flows. The effects of turbulence are included using turbulence models. The finite volume method is used to discretize the equations in time and space. The principle of the finite volume method is to divide the flow region into a large number of control volumes. These control volumes can be of different shapes, but they are often chosen to be hexahedral (six faces), to reduce the numerical errors and convergence problems. The totality of these control volumes is called the computational grid, or mesh. The viscous fluid flow equations, including a turbulence model, are then solved, and the different flow properties are computed at the centre of each control volume. Doing so, the flow features inside a water turbine can be solved. To predict the flow features accurately, a large number of control volumes is needed, making the computational grid very large. To compute such a domain, a lot of computational resources is required, in term of CPU time and RAM memory, and it usually takes a long time to compute. However, the computational technology has greatly improved the last decades. The CPU speed is much faster and RAM and cache memory more than doubled compared to 10 years ago. This permits to simulate larger and larger cases and to predict flow features that could not be computed previously.

To numerically simulate the flow in a domain, it is required to specify the conditions at the boundaries of the flow region such as the inlet, the walls and the outlet. The flow features predicted by the equations that govern the flow will largely depend on the quality of the boundary conditions. If the boundary conditions are not correct, the prediction of the flow will be less accurate. The Turbine-99 workshops showed that it is very important to take into account the radial velocity at the inlet of a draft tube to get a good prediction of the flow in the draft tube [3]. To correctly predict the flow features in the draft tube, the inlet boundary condition should be chosen further upstream, i.e. the runner should be included in the simulations [4].

It is similar when specifying the conditions at the inlet of the spiral casing. Much attention has been directed to runners and draft tubes, while few have focused on the spiral casing. It is common to ignore the effects of the shape of the penstocks and to set a constant velocity at the inlet of the spiral casing. However, Mulu et al. [5] showed that without accounting for the flow features in the penstocks, the predicted flow in the spiral casing and thus in the runner is not correct. Similarly, the walls and outlet boundary conditions play a big role in the numerical results and can be the reason to a diverging simulation, or to a wrong prediction of the flow features.

The turbulence model used to solve the flow equations is also very important for the accuracy of the results. Basic models such as the k-ε model allow a more stable computation, but do not predict accurately all the turbulence. Depending on the geometry of the domain, and on the flow behavior inside this domain, some turbulence models are more suitable than other. In a draft tube, Gyllenram [6] showed that a limit of the modeled scales can be used to predict the turbulent flow features with better accuracy. With this approach, more scales are resolved in time and space. Because it is time-consuming and expensive to numerically resolve all scales of motion in the flow, different approaches to turbulence modeling can be chosen. The fastest and least accurate methods are the steady RANS (Reynolds Average Navier Stokes) equations. Because they are based on solving the time-averaged Navier-Stokes equations, the unsteadiness of the flow will not be solved. The turbulence model will then have to predict all the unsteady flow features, thus the turbulence model needs to be advanced. However, steady RANS simulations do not require a long computational time, and the prediction of the overall flow is reasonably good. Unsteady RANS simulations show a good potential to predict the large scale unsteadiness [7]. It takes a longer time to compute, as another dimension (time) is added. To predict the small-scale turbulence, Large Eddy Simulation (LES) and Direct Numerical Simulation (DNS) methods are used. However, it requires a much finer grid resolution, and a lot of computing time. For water turbines, steady RANS and unsteady RANS methods are two common methods used to investigate the whole system.

Since some parts of the water turbine rotate (runner) while the rest is steady (spiral casing and draft-tube), a rotor-stator approach is necessary to predict the flow in the whole system. The *frozen rotor* approach is a steady-state formulation where the rotor and stator are fixed with respect to each other, and different frames of reference are used in the rotating and stationary parts. This allows taking into account the effect of the rotation of the runner, although no transient interaction is included. Petit et al. [8] showed that the steady RANS method using the frozen rotor approach gives a general understanding of the flow for rotor stator applications. However, the advection of the wakes of the rotor through the stator is physically incorrect, and Petit et al. showed that unsteady RANS simulations give much better results.

Because of all those approximations, numerical simulations can give an inaccurate prediction of the flow features. To assert the credibility of tur-

bulence models, boundary conditions or methods, it is necessary to validate the computational technique against detailed measurements. Due to the difficulty often faced when doing measurements in real scale turbines, detailed databases are often performed on reduced case models. The FLINDT project [9] created a detailed database on the unsteadiness of the flow in a draft tube, and the creation of the precessing vortex rope. This project served as a validating database for computational techniques [10], but is not publically available. For the validation of OpenFOAM, the ERCOFTAC case-studies [11, 8] served as a validation database for new turbomachinery applications within OpenFOAM, such as the General Grid Interface [12]. The present work presents yet another validation test case of a free runner swirl generator.

Scope of the Present Work

The use of computational fluid dynamics (CFD) to numerically investigate the flow of water through water turbines has become increasingly popular the last decades. Its flexibility, detailed flow description and cost-effectiveness makes it an attractive alternative to experimental investigations. It is nowadays widely used in the design and refurbishment process, and to get a good understanding of the flow in the water turbine for different operating conditions. However, issues still have to resolved due to the combined physics involved in a water turbine, such as vortices, unsteadiness in the draft tube or swirling flow. Predicting the flow in water turbines requires a lot of computational resources. Running a simulation only on one CPU, when possible, takes a very long time for most cases. The computational speed can though be increased by using several CPUs simultaneously, and computing different parts of the problem on different CPUs. The memory requirement to solve the equations on the discretized region is thus also distributed between the different CPUs. When using a commercial software, parallel simulations require many licenses, which tend to be costly.

In the present work, the relatively new OpenFOAM CFD tool was used. The OpenFOAM® CFD solver was released as Open Source software in the end of 2004. It is a C++ object-oriented library for numerical simulations of partial differential equations [13]. Due to the OpenSource distribution under the GPL license, it can be used at no cost. The OpenFOAM community is growing every year, and contributes to the development of this software. Since it is still a rather new CFD tool, there is a need to develop and validate some features. It is an important part of this work to develop and validate turbomachinery applications, and to make it available and useful for the community through different case studies.

The main goal of the present work is to correctly predict the flow in the U9 Kaplan water turbine. At design phase of the U9 prototype, the effect on the flow of the penstock curvature at the inlet of the spiral casing was not taken into account. A previous study shows that this induces an error in the predicted flow [5]. It is the main goal of this work to investigate the choices of boundary conditions and to find the one that predicts the flow features as accurately as possible. To make sure that the predicted flow is in good agreement with the real flow, a broad range of validating measurements must be available. Because doing measurements on a real-scale water turbine is time and money consuming, a 1:3.1 scaled model of the U9 unit was experimentally investigated at VattenFall Research and Development in

Älvkarleby, Sweden [14, 15, 16]. The U9 turbine is composed of 6 runner blades, 20 guide vanes, and 18 stay vanes, and has a runner diameter of 0.5m. However, due to the complexity of the computational domain, it is essential to validate the computational techniques on simpler geometries. The present work thus includes two other case studies, with access to detailed experimental databases, used to validate the computational techniques. The results and experiences obtained for those two case-studies were released and shared to the community as a guide on how to simulate turbomachinery applications in OpenFOAM.

The two different case studies are presented below:

- The ERCOFTAC Centrifugal Pump [8] was used to validate a new functionality in OpenFOAM, the General Grid Interface (GGI) [12]. A GGI is commonly used in turbomachinery, where the flow is simulated through a succession of various complex geometries. The requirement to fit all meshes with conformal matching interfaces is often very hard to reach. Using the GGI, non-conformal meshes can be designed separately, and joined together. Rotor-stator interaction, steady and unsteady RANS method are validated as well. This case-study was released and shared with the community to guide new OpenFOAM users on how to get accurate results efficiently using those applications. Detailed measurements of the flow are available [17], making this case study a very good case to validate the computational technique generally use in turbomachinery applications.

- The Timisoara swirl generator case-study [18] presents a computational domain that has similar parts as a water turbine, that is to say guide vanes, runner and draft tube. This is thus a very good case to validate the computational technique used in the U9 turbine simulations. The test rig was designed at Politehnica University of Timisoara, Romania, to experimentally investigate the vortex rope that forms at part discharge below the runner [18]. The flow is thus very turbulent, and is a very good case study to investigate the impact of the boundary conditions and of the turbulence model on the prediction of the turbulent flow features.

Bibliography

[1] D. Böhme, W. Dürrschmidt, and M. Van Mark, editors. *Renewable Energy Sources in Figures - National and International Development.* Federal Ministry for the Environment, Nature Conservation and Nuclear Safety (BMU), Public Relations Division, 2009.

[2] M.J. Cervantes, I. Jansson, A. Jourak, S. Glavatskikh, and J.O. Aidanpää. Porjus U9, a Full-scale Hydropower Research Facility. *24^{rd} IAHR Symposium on Hydraulic Machinery and Systems - Foz Do Iguassu*, 2008.

[3] M.J. Cervantes, L.H. Gustavsson, M. Page, and F. Engström. Turbine-99, a Summary. *23^{rd} IAHR Symposium - Yokohoma*, 2006.

[4] T.C. Vu, B. Nennermann, G.D. Giocan, M.S. Iliescu, O. Braun, and F. Avellan. Experimental Study and Unsteady simulation of the FLINDT Draft Tube Rotating Vortex Rope. *Hydro - Porto*, 2004.

[5] B. Mulu and M. Cervantes. Effects of Inlet Boundary Conditions on Spiral Casing Simulation. *Scientific bulletin of the "Politehnica" University of Timisoara Transactions on Mechanics*, Tom 52(66), Fascicola 6, 2007.

[6] W. Gyllenram. *Analytical and Numerical Studies of Internal Swirling Flows.* PhD thesis, Division of Fluid Dynamics, Chalmers University of Technology, 2008.

[7] S. Muntean, H. Nilsson, and R.F. Susan-Resiga. 3D Numerical analysis of the unsteady turbulent swirling flow in a conical diffuser using Fluent and OpenFOAM. *3^{rd} IAHR International Meeting of the Workgroup on Cavitation and Dynamic Problems in Hydraulic Machinery and Systems - Brno*, 2009.

[8] O. Petit, M. Page, M. Beaudoin, and H. Nilsson. The ERCOFTAC Centrifugal Pump OpenFOAM Case-Study. *3^{rd} IAHR International Meeting of the Workgroup on Cavitation and Dynamic Problems in Hydraulic Machinery and Systems - Brno*, 2009.

[9] F. Avellan. Flow investigation in a Francis draft tube: the FLINDT project. *IAHR Symposium on Hydraulic Machinery and Systems*, 2000.

[10] R.F. Susan-Resiga, S. Muntean, C. Tanasa, and A. Bosioc. Hydrodynamic Design and Analysis of a Swirling Flow Generator. *4^{th} German-Romanian Workshop on Turbomachinery Hydrodynamics, GROWTH-4 - Germany*, 2008.

[11] H. Nilsson, M. Page, M. Beaudoin, and H. Jasak. The OpenFOAM turbomachinery working group, and conclusions from the turbomachinery session of the third OpenFOAM Workshop. *3^{rd} IAHR International Meeting of the Workgroup on Cavitation and Dynamic Problems in Hydraulic Machinery and Systems - Brno*, 2009.

[12] M. Beaudoin and H. Jasak. Development of a Generalized Grid Interface for Turbomachinery Simulations with OpenFOAM. *Open Source CFD International Conference - Berlin*, 2008.

[13] H.G. Weller, G. Tabor, H. Jasak, and C. Fureby. A Tensorial Approach to Computational Continuum Mechanics using Object-Oriented Techniques. *Computers in physics*, Vol.12(No.6), 1998.

[14] B. Mulu and M. Cervantes. Experimental Investigation of a Kaplan model with LDA. *33^{rd} IAHR Congress: Water Engineering for a Sustainable Environment*, 2009.

[15] B. Mulu and M. Cervantes. LDA Measurements in a Kaplan Spiral Casing Model. *13^{th} International Symposium on Transport Phenomena and Dynamics of Rotating Machinery*, 2010.

[16] P. Jonsson and M. Cervantes. Time Resolved Pressure Measurements on a Kaplan Model. *33^{rd} IAHR Congress: Water Engineering for a Sustainable Environment*, 2009.

[17] M. Ubaldi, P. Zunino, G. Barigozzi, and A. Cattanei. An Experimental Investigation of Stator Induced Unsteadiness on Centrifugal Impeller Outflow. *Journal of Turbomachinery*, vol.118, 41-54, 1996.

[18] A.I. Bosioc, C. Tanasa, S. Muntean, and R.F. Susan-Resiga. 2D LDV Measurements of Swirling Flow in a Simplified Draft Tube. *The 14^{th} International Conference on Fluid Flow Technologies*, 2009.

Summary of Papers

Paper I

The Flow in the U9 Kaplan Turbine - Preliminary and Planned Simulations using CFX and OpenFOAM.

Paper I reports a numerical study of the flow in the U9 spiral casing and draft tube. The time-averaged Reynolds-Averaged Navier Stokes equations (RANS) are solved, using the finite volume method and the standard k-ε turbulence model closure with wall-functions. Two different computational domains were realized, one for the draft tube and one for the spiral casing. The simulations were done separately. The two computational grids used to define the domains are unstructured, with tetrahedral cells. OpenFOAM and CFX give similar results for the spiral casing as well as for the draft tube, though the pressure loss in the spiral casing differs a bit between the two codes. Paper I shows that OpenFOAM gives similar results as a commercial CFD software, and that it is a viable CFD software choice for this work.

Paper II

The ERCOFTAC Centrifugal Pump OpenFOAM Case-Study.

Paper II presents and validates the implementation of the General Grid Interface (GGI) in OpenFOAM, as well as two different methods used in turbomachinery to predict the flow features: the frozen-rotor steady state method, and the sliding grid unsteady method. Both methods are widely used when predicting the flow features in turbomachinery applications, but few detailed case studies are available in OpenFOAM. The ERCOFTAC centrifugal pump is a good test case for validating rotor-stator interaction features, as detailed experimental results are available. Paper II shows that the steady-state frozen rotor method gives a good overview of the flow, but does not predict the advection of the runner wakes properly, which on the other hand is done well by the sliding grid method. The results of this work were presented at the 4^{th} OpenFOAM Workshop held in Montreal, Canada in June 2009. The case study is now available to everyone as a tutorial, and can be found online.

Paper III

Comparison of Numerical and Experimental Results of the Flow in the U9 Kaplan Turbine Model.
(Extended version to be submitted to IAHR 2010)

Paper III compares simulations made using OpenFOAM with experimental measurements of the flow in the U9 Kaplan turbine model. The focus of the paper is on the flow in the spiral casing and in the draft tube. The two computational domains are done using ICEM-Hexa, and the meshes are block-structured. The numerical results were obtained using the finite volume method and the standard k-ε turbulence model. The two computational domains were simulated separately. For the spiral casing, the 2D LDV measured velocity profiles are compared with the numerical results at three different positions. The numerical results in the spiral casing are in good agreement with the measurements, but they also show that there is room for improvement by changing the turbulence model and improving the inlet boundary conditions. The predicted flow in the draft tube is in good agreement with the experimental data. However, improvements can also be made by changing the inlet boundary condition and taking into account the radial velocity and the asymmetric and unsteady behaviour of the flow at the inlet of the draft tube.

Paper IV

A Swirl Generator Case Study for OpenFOAM - Experimental and Numerical Validation.
(Extended version to be submitted to IAHR 2010)

Paper IV validates numerical results of the flow in the swirl generator test rig located in Politehnica University of Timisoara, Romania. The test rig is a simplified turbine that aims at studying the precessing vortex rope that is created after a runner when operated at partial discharge. 3D unsteady simulations using the sliding grid method are compared to experimental results and numerical Mixing Interface results from Fluent. The comparison shows that the flow predicted by OpenFOAM is in good agreement with the measured flow and with commercial CFD softwares, and that turbulence features are accurately predicted. It seems however that to get the full turbulence features of the flow, a better turbulence model should be used.

Paper I

IAHR
24th Symposium on Hydraulic Machinery and Systems
OCTOBER 27-31, FOZ DO IGUASSU

THE FLOW IN THE U9 KAPLAN TURBINE - PRELIMINARY AND PLANNED SIMULATIONS USING CFX AND OPENFOAM

AUTHORS

Olivier Petit[(1)], Håkan Nilsson[(1)], Thi Vu[(2)], Ovidiu Manole[(2)], Svante Leonsson[(3)]

[1] Chalmers University of Technology, Sweden
[2] Andritz VA Tech Hydro Ltd., Canada
[3] Andritz Hydro Inepar Sweden AB
Corresponding author: Olivier Petit, olivierp@chalmers.se

ABSTRACT

The present work compares the CFX and OpenFOAM CFD codes with respect to the prediction of the flow in the U9 Kaplan turbine spiral casing, distributor and draft tube. The simulations use similar settings and the same computational grids – unstructured wall-function grids with 10.3M cells in the spiral casing and distributor, and 1.04M cells in the draft tube. The results show that the two codes give similar results in the spiral casing and distributor, and almost identical results in the draft tube. Previous studies [1] have shown the same behaviour in the Turbine-99 draft tube, for a block-structured wall-function grid. There are however no previous studies where the flow in a spiral casing and distributor have been studied and compared using the same settings and computational grid in CFX and OpenFOAM.

The next phase of the project consists of comparisons with the results from an on-going experimental investigation.

KEY WORDS: CFD, Water Turbine, Draft Tube, Spiral Casing, Distributor, CFX, OpenFOAM

INTRODUCTION

The U9 Kaplan turbine is a unique combination of model and full scale research units. The full scale turbine is located in Porjus, in the most northern parts of Sweden, and the model scale turbine is located at Vattenfall Research and Development in Älvkarleby, in the center of Sweden. The present paper describes the initial work done, and the planned activities, in a newly started PhD and collaboration project regarding simulations of the flow in the U9 Kaplan turbine. CFX simulations are being done at Andritz VA Tech Hydro Ltd. (Canada), and OpenFOAM simulations are being done at Chalmers University of Technology, Sweden. With similar settings for the simulations and using the same computational grid it is possible to compare different aspects of the simulations, such as accuracy, efficiency and general features of the two codes. Detailed measurements of the flow in both model and full scale will be made in other PhD projects, and those measurements will be used to validate the computational results.

The present paper shows preliminary computational results from CFX and OpenFOAM, of the flow in the U9 spiral casing, distributor, and draft tube. Andritz Hydro Inepar Sweden AB has designed and provided the geometrical information. Andritz VA Tech Hydro Ltd. (Canada) has provided the CAD models, the grids, and the CFX computations. The OpenFOAM computations have been done at Chalmers. The preliminary results show that CFX and OpenFOAM give similar results, but with some significant differences. Further work will be done in order to find out the reason for the differences, and to propose how to minimize the differences in order to get the most accurate results.

In this initial phase of the project the focus has been on the flow in the spiral casing, distributor and draft tube. Soon also the runner, and the coupling between the different parts of the system will be studied. One of the main aims of the project is to study the influence of different choices of boundary conditions on the computed flow. As an example, in both the model and full scale there is a 90 degree bend on the inlet pipe at approximately 5 diameters before the inlet of the spiral casing. The influence of this bend on the flow throughout the turbine will be studied. Internal boundary conditions, such as rotor-stator interfaces, and GGI interfaces will also be studied.

METHODOLOGY

Both the CFX and OpenFOAM CFD codes use similar approaches to solve for the velocity, pressure, and modeled turbulence fields. The basis is the Finite Volume Method, where the computational domain is divided into a large number of polyhedral control volumes (cells) in which the equations are discretized and solved iteratively. In the present work the computational grids consist of a mix of tetrahedral, pyramid and prism cells. The prism cells are used in the boundary layers in order to increase the accuracy of the results in those regions where there are large gradients. The effect of turbulence is modeled using the standard k-ε turbulence model. All the computations in the present work are steady. Boundary conditions for all the variables must be set at all the outer boundaries, and discretization schemes must be specified in order to complete the set-up of the problem. Those settings are described below for each of the two cases. The name of the OpenFOAM solver is simpleFoam, and the version of OpenFOAM is 1.4.1. The version of CFX is 10.0 SP1.

Description of the U9 spiral casing and distributor case

Figure 1 shows a view of the computational domain of the U9 spiral casing and distributor. The geometry has been scaled to correspond to a runner throat diameter of 1m in this study. There are 10.3M control volumes in the unstructured grid. The final near-wall grid resolution corresponds to an average $y^+ = 35$, and standard wall-functions are used at the walls.

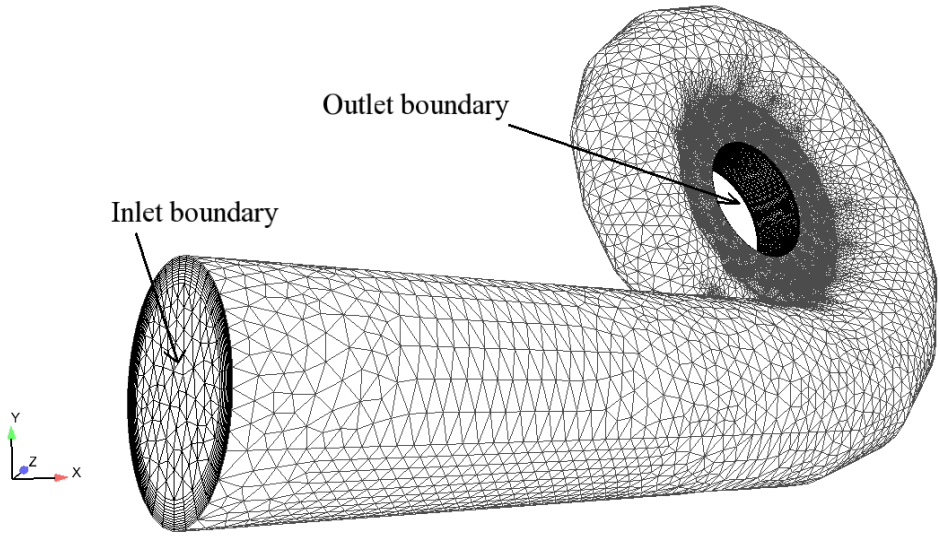

Figure 1: The spiral casing and distributor computational domain and unstructured grid

Constant inlet values are specified for the velocity and turbulence quantities. The turbulence intensity, I, is 2%, and the turbulence length scale is given by the viscosity ratio ν_t/ν=50. The values are given by $\mathbf{U}$=[1.88727, 0, 0]m/s, $k=1.5(U_x*I)^2 m^2/s^2$, and $\varepsilon=C_\mu\ k^2/((\nu_t/\nu)\ \nu) m^2/s^3$. The Neumann boundary condition is used for the velocity and turbulence quantities at the outlet. For the static pressure, the Neumann boundary condition is used at all boundaries, but the level of the static pressure is corrected by setting the average outlet static pressure to zero.

The convection terms in the Navier-Stokes equations are discretized using the GammaV discretization scheme [2] in OpenFOAM, while the "High Resolution" discretization scheme has been used in CFX.

Description of the U9 draft tube case

Figure 2 shows the computational domain of the U9 draft tube. The geometry has been scaled to correspond to a runner throat diameter of 1m in this study. There are 1.04M control volumes in the unstructured grid. The final near-wall grid resolution corresponds to an average y^+ = 231, and standard wall-functions are used at the walls.

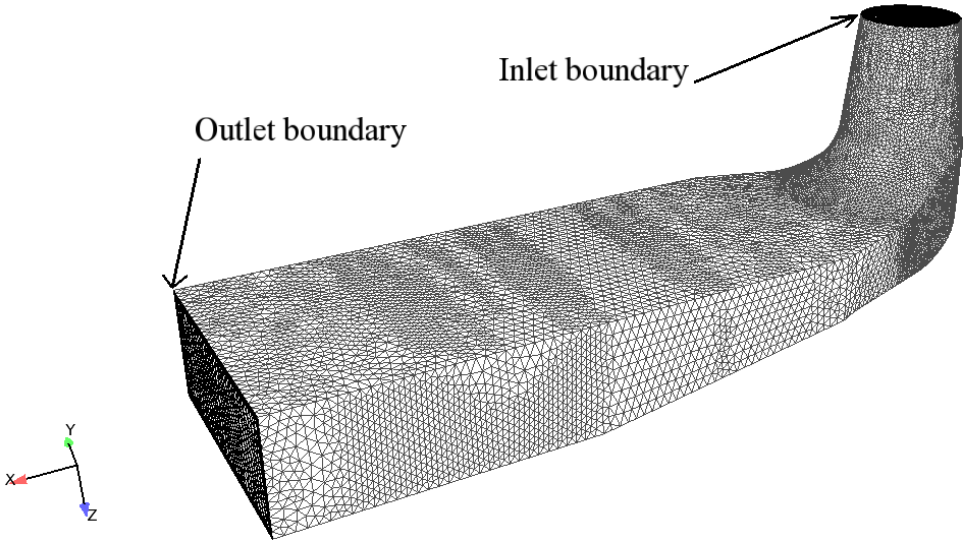

Figure 2: The U9 draft tube computational domain and unstructured grid

At the inlet a solid-body swirl is applied since there are yet neither experimental nor computational results available at that cross-section. The turbulence intensity, I, is 5%, and the turbulence length scale is given by the viscosity ratio ν_t/ν=100. Neumann boundary conditions are used at the outlet. For the static pressure, the Neumann boundary condition is used at all boundaries, but the static pressure level is corrected by setting the average outlet static pressure to zero.

The convection terms in the Navier-Stokes equations are discretized using the GammaV discretization scheme [2] in OpenFOAM, while the "High Resolution" discretization scheme has been used in CFX.

RESULTS

The computational results are first compared and discussed for the spiral casing and distributor, and then for the draft tube.

The spiral casing and distributor

Here the results from the CFX and OpenFOAM simulations of the flow in the U9 spiral casing and distributor are compared. The integrated losses are compared between the three cross-sections shown in Figure 3. The velocity and modeled turbulence are compared along the inlet and outlet lines, which are also shown in Figure 3. In the evaluation of the losses the *Spiral Casing* is defined between the cross-sections referring to the *inlet of the spiral casing*, and the *inlet of the distributor*. The *Distributor* is defined between the cross-sections referring to the *inlet of the distributor*, and the *outlet of the distributor*.

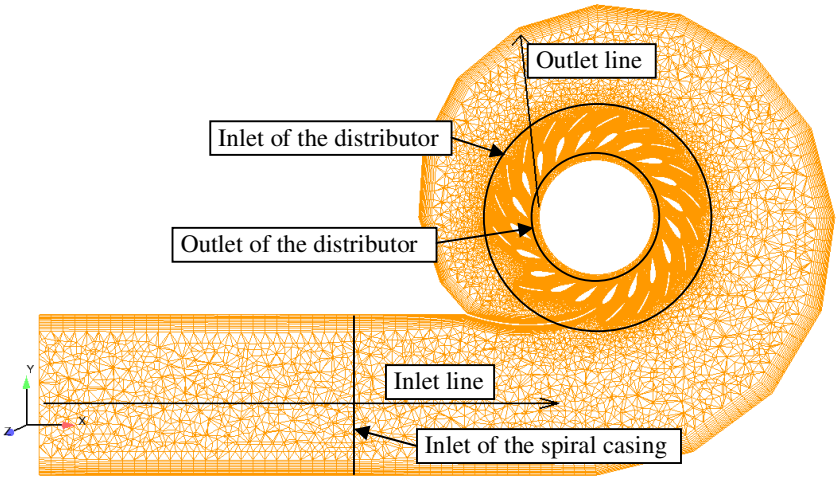

Figure 3: Locations of the three cross-sections, and the inlet and outlet comparison lines

Table 1 shows the integrated losses in the *Spiral Casing* and the *Distributor*. The losses are defined as $Loss = \frac{\Delta P_{tot}}{\frac{1}{2} * \rho * v_{Throat}^2} * \frac{1}{Q_{11}^2} * 100$, where ΔP_{tot} is the change in mass-flow averaged total pressure between the two cross-sections. $Q_{11} = \frac{Q * \sqrt{2 * g}}{D_{Throat} * v_{Throat}} = \frac{v_{Throat} * A_{Throat}}{D_{Throat} * v_{Throat}} * \sqrt{2 * g} = \pi * \sqrt{\frac{g}{2^3}}$ is the reduced discharge, where subscript *Throat* refers to the runner cross-section. The major difference between the results of the two codes with respect to the loss is in the *Spiral Casing*, although that is more or less flow in a curved channel. The properties of the simulations that are mostly affecting the predicted losses in this region are the near-wall modeling, the turbulence modeling, and the numerical diffusion due to the choice of convection discretization scheme. The

reason for the difference will be examined thoroughly in future work, but a small preliminary discussion will also be made when comparing the static pressure results along the outlet line.

	Loss from CFX (%gH)	Loss from OpenFOAM (%gH)
Spiral Casing	0.10146	0.27687
Distributor	0.31322	0.390207
Total	0.414679	0.667086

Table 1: Losses computed in CFX and OpenFOAM

Figure 4 shows comparisons of the distributions of velocity magnitude and static pressure along the inlet line and outlet line shown in Figure 3. The results from the two codes are very similar, although there are some significant differences. The most obvious difference is the static pressure level in the spiral casing, along the inlet line, and at the outer part of the outlet line. The difference in static pressure is rather constant in those regions. However, at the cross-section at the inlet of the distributor (Abscissa ~0.62) the two codes give identical results both for the static pressure and the velocity magnitude, and thus also for the total pressure. This suggests that the main contribution to the difference in the loss from the two codes originates in the region where the flow enters the distributor. That region is part of the evaluation of the loss in the *Spiral Casing*, which is then blamed for the difference although the difference seems to be much more localized to the inlet of the distributor. This will be investigated thoroughly in the near future.

Figure 5 shows comparisons of the distributions of turbulent kinetic energy and turbulence dissipation along the inlet line and outlet line shown in Figure 3. The differences in the turbulence properties are significant, but not unexpected. The turbulence properties are very sensitive, and the small differences we see in the velocity distribution give slightly different flow direction and velocity gradients, which may give large differences in the modeling of the turbulence. It can only be concluded that the results are identical along the inlet line, and show qualitative similarity at the outlet line with respect to the turbulence quantities.

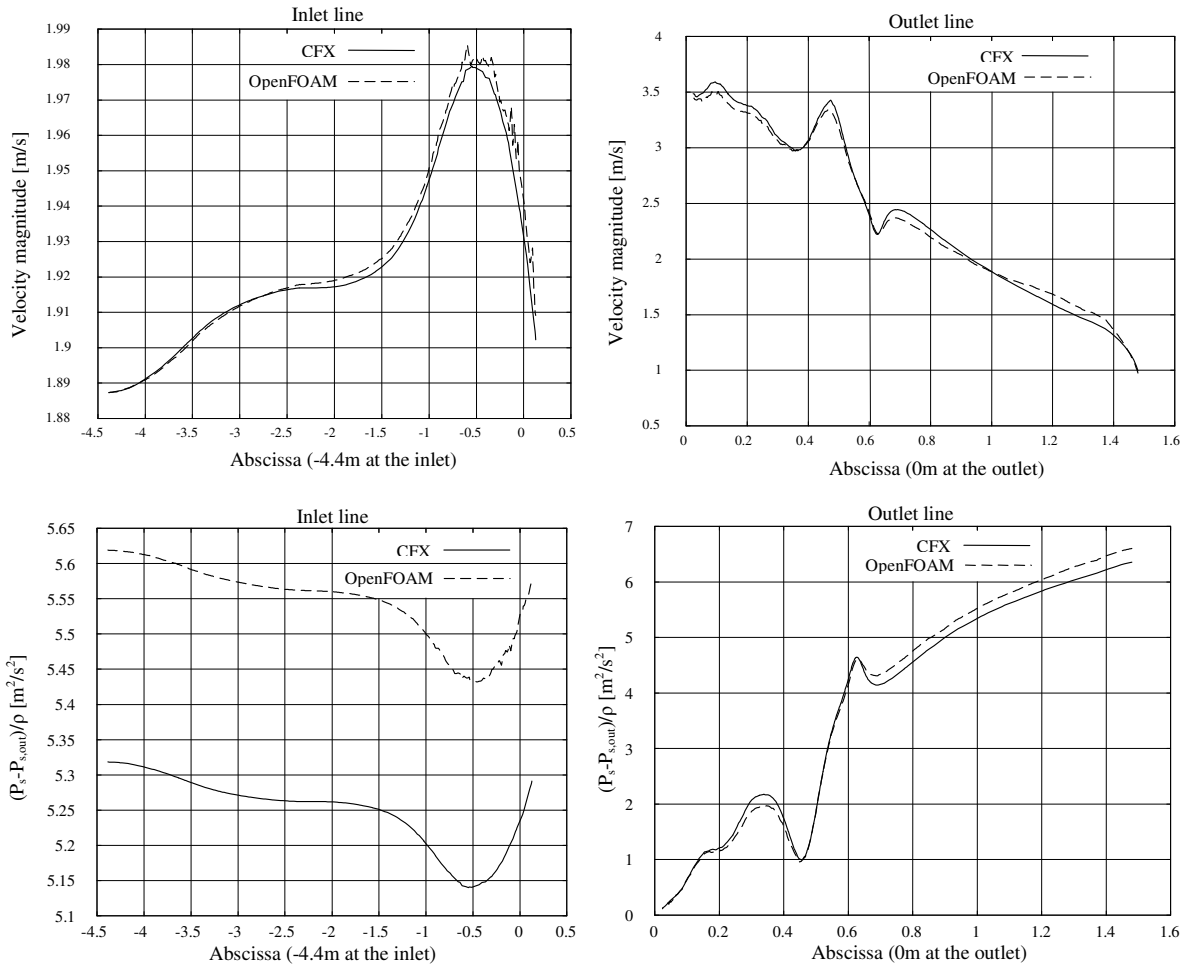

Figure 4 Static pressure, represented by $(P_s-P_{s,out})/\rho$, and velocity magnitude in the spiral casing and distributor, computed by CFX and OpenFOAM. Note that the difference in the static pressure at the inlet line is amplified by the choice of y-axis scaling. The difference at the inlet is similar as that at Abscissa ~1m along the outlet line.

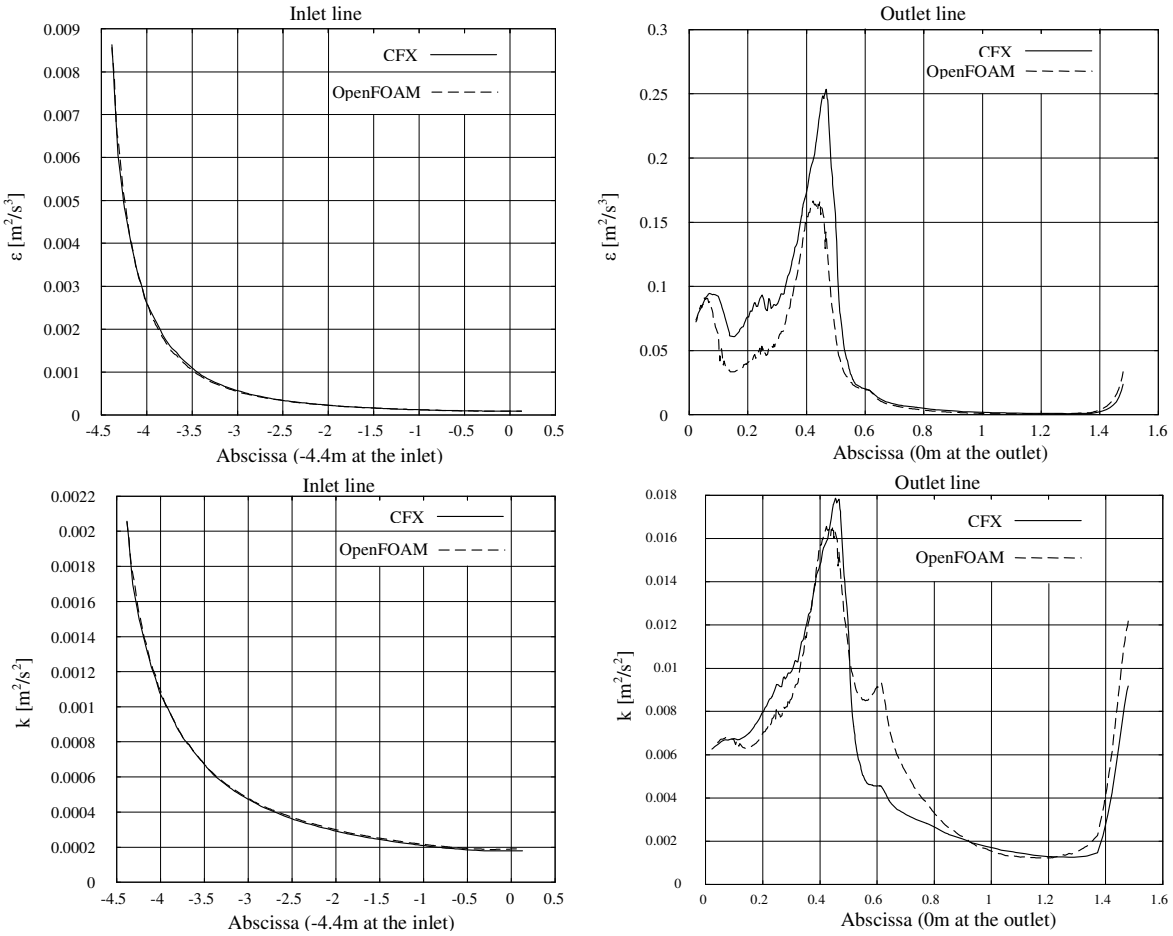

Figure 5 Turbulence properties in the spiral casing and distributor computed by CFX and OpenFOAM

The Draft Tube

Here the results from the CFX and OpenFOAM simulations of the flow in the U9 draft tube are compared. The comparisons are made with respect to the distribution of the static pressure along the upper centerline, shown in Figure 6, and contours of the static pressure and velocity magnitude at the center plane and at a cross-section of the draft tube.

Figure 6 shows the difference in predicted static pressure from CFX and OpenFOAM along the upper center line. The static pressure is set to zero at the outlet. The results from CFX and OpenFOAM are almost identical.

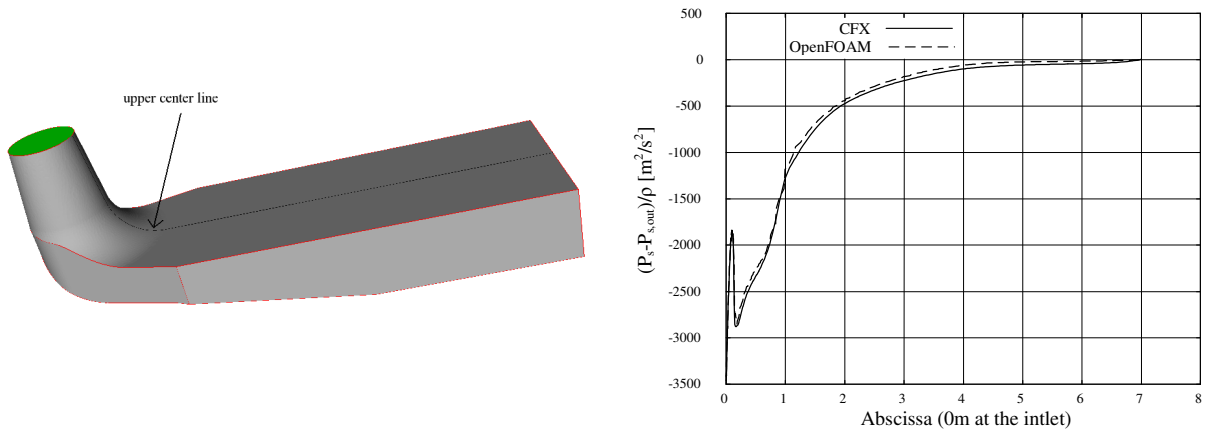

Figure 6: Static pressure computed by CFX and OpenFOAM along the upper center line

Figure 7 compares the CFX and OpenFOAM results with respect to the static pressure distribution at the center plane. The results are almost identical. It can be seen that the static pressure is reduced in the center of the inlet vortex, and that the static pressure gradient is responsible for re-directing the flow in the elbow. It can also be seen that the static pressure is recovered (increased) as the water flows through the draft tube.

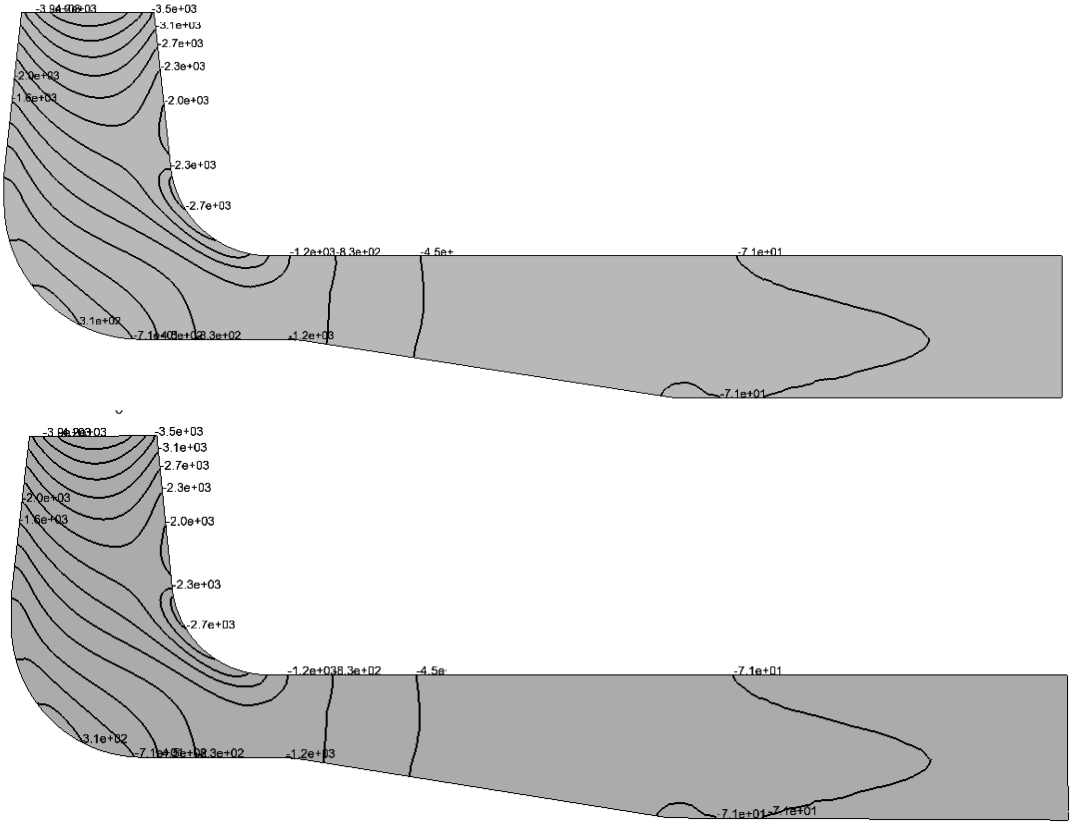

Figure 7: Static pressure contours computed by CFX (top) and by OpenFOAM (bottom)

Figure 8 shows contour lines of the velocity magnitude at the draft tube outlet. The results from the two codes are identical.

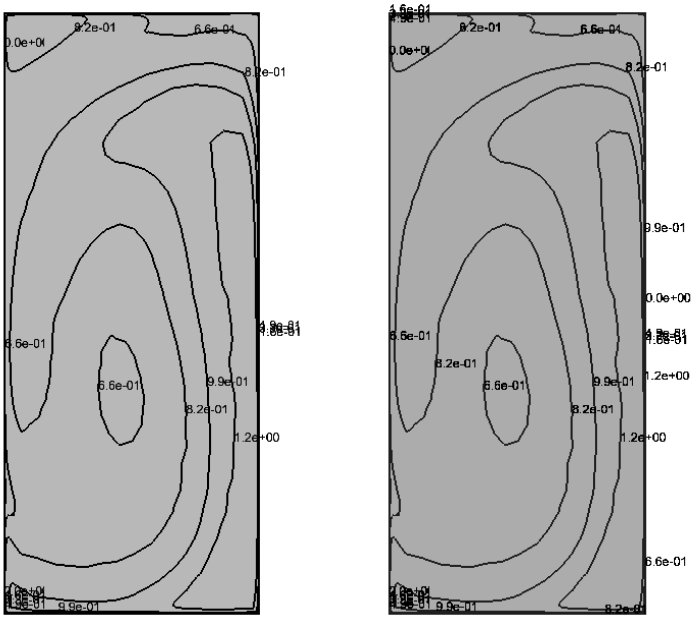

Figure 8: Velocity contours at the draft tube outlet, computed by CFX (left) and by OpenFOAM (right). The view is in the streamwise direction, and the vertical upward direction is to the right.

FUTURE WORK

The next phase of the project consists of comparisons with the results from an on-going experimental investigation of the U9 model. There will be detailed comparisons at the inlet of the spiral casing, in the spiral casing, in the distributor, in the runner, and in the draft tube.

The results presented in this paper are restricted to one unstructured grid for each of the two cases. Block-structured grids are usually used when computing the flow in water turbines in order to increase the accuracy of the results. A fully structured grid for the spiral casing and distributor case has been generated at Chalmers, and the same comparisons will be made using that grid. Furthermore, a grid resolution study should be made.

Also the runner, and the coupling between the rotating and non-rotating parts of the system, will be studied. For this to be possible in OpenFOAM there is a need for some implementations and validations of those implementations.

When it has been verified that both CFD codes give similar results as the experimental results, the main aim is to study the influence of different boundary conditions. Initially the effect of a 90 degree bend before the inlet of the spiral casing will be studied. Such a 90 degree bend is present in the U9 model and prototype, and it is important to investigate how this will influence the details of the flow throughout the turbine.

ACKNOWLEDGEMENTS

We would like to acknowledge the Swedish Water Power Center, SVC, which financed the present work. SVC has been established by the Swedish Energy Agency, ELFORSK and Svenska Kraftnät together with Chalmers University of Technology, Luleå University of Technology, Uppsala University and the Royal Institute of Technology.

We would also like to acknowledge the OpenFOAM community, and in particular Maryse Page and Martin Beaudoin, Hydro Quebéc, in the OpenFOAM Turbomachinery Working Group[3], for fruitful exchange of best-practice guidelines, and for sharing OpenFOAM implementations.

The OpenFOAM simulations in this work has been made on clusters financed by SNIC, the Swedish National Infrastructure for Computing, whom we greatfully acknowledge.

REFERENCES

[1] H.NILSSON AND M.PAGE, December 8-9 2005, *OpenFOAM simulation of the flow in the Hölleforsen draft tube model*, Turbine-99 III, Porjus, Sweden

[2] H.JASAK, H.G.WELLER, AND A.D.GOSMAN, 1999, *High resolution NVD differencing Scheme for Arbritarily Unstructured Meshes*, International Journal for Numerical Methods in Fluids, p.431-449

[3] H.NILSSON, M.PAGE, M.BEAUDOIN, B.GSCHAIDER, H.JASAK, October 27-31 2008*, The OpenFOAM Turbomachinery Working Group, and conclusions from the turbomachinery session of the third OpenFOAM workshop*, 24th IAHR Symposium, Foz do Iguassu, Brazil

Paper II

The ERCOFTAC centrifugal pump OpenFOAM case-study

Olivier PETIT

Chalmers University of Technology, Göteborg, Sweden

Maryse PAGE

Hydro-Québec, Institut de recherche, Varennes, Canada

Martin BEAUDOIN

Hydro-Québec, Institut de recherche, Varennes, Canada

Håkan NILSSON

Chalmers University of Technology, Göteborg, Sweden

ABSTRACT

This work investigates the rotor-stator interaction features of OpenFOAM-1.5-dev, such as frozen rotor and sliding grid. The case studied is the ERCOFTAC *Test Case U3: Centrifugal Pump with a Vaned Diffuser*, a testcase from the ERCOFTAC Turbomachinery Special Interest Group. The case was presented by Combès at the *ERCOFTAC Seminar and Workshop on Turbomachinery Flow Prediction VII*, in Aussois, 1999. It is a valid test case for evaluation of rotor-stator interaction features, as detailed experimental data is available.

The investigation shows that OpenFOAM gives results that are comparable to the experimental data, in particular for the sliding grid case. The results are less accurate in the frozen rotor simulation due to the improper treatment of the impeller wakes that is part of the frozen rotor formulation.

The ERCOFTAC centrifugal pump OpenFOAM case-study was developed as a contribution to the OpenFOAM Turbomachinery Working Group, and was presented and discussed at the Fourth OpenFOAM Workshop in Montréal, 2009. The complete set-up of the case-study is available from the OpenFOAM-extend project at SourceForge, and instructions and comments are available from the OpenFOAM Wiki.

KEYWORDS

CFD, OpenFOAM, Turbomachinery, Frozen rotor, Sliding grid, GGI, ERCOFTAC centrifugal pump

1 INTRODUCTION

OpenFOAM is an Open Source library written in C++ [1]. It is a well-structured code, mostly used to implement CFD solvers, although it is also used in other applications. OpenFOAM is based on the finite volume method, but there are also implementations of the finite area and finite element methods. The code accepts fully unstructured meshes and polyhedral cells. Many advanced features can be found in OpenFOAM, such as moving meshes and conjugate heat transfer. With regards to basic features, such as turbulence models and discretization schemes, OpenFOAM is a serious and high quality CFD tool that is constantly evolving.
The community-driven OpenFOAM Turbomachinery Working Group [2] develops and validates OpenFOAM for turbomachinery applications. The ERCOFTAC centrifugal pump was chosen as a validation test case for this investigation of the rotor-stator interaction features in OpenFOAM. The results of the initial studies of this case were presented at the Fourth OpenFOAM Workshop in June 2009, in Montréal, Québec. All the files are available at the OpenFOAM-extend project at SourceForge, for anyone who would like to learn OpenFOAM, or become familiar with the turbomachinery features in OpenFOAM. Some of the important features, such as the GGI (General Grid Interface), multiple frames of reference, and moving meshes are described in the present paper. The GGI forms the base for many useful features for turbomachinery.

2 METHOD

In this work, the flow through a centrifugal pump is investigated. The incompressible Reynolds-Averaged Navier-Stokes equations are solved, using the finite volume method and a standard k-ε turbulence model closure with wall-functions. The convection discretization uses a second-order linearUpwind scheme. Two different rotor-stator approaches are used:

- The *frozen rotor* approach is a steady-state formulation where the rotor and stator are fixed with respect to each other, and different reference frames are used in the rotating and stationary parts. This is also referred to as Multiple Reference Frames (MRF), and it allows taking into account the effect of the rotation of the impeller, although no transient rotor-stator interaction is included. It is nevertheless a fast preliminary method, for use as initial conditions for sliding grid simulations.
- The *sliding grid* approach is a transient method where the rotor mesh actually rotates with respect to the stator mesh. The interaction between the rotor and stator are thus fully resolved. This requires a sliding grid interface between the rotor and stator domains. In OpenFOAM there are two alternatives for sliding interfaces, GGI and topology changes.

Details on the two approaches can be found in section 4.

3 THE ERCOFTAC CENTRIFUGAL PUMP CASE-STUDY

The ERCOFTAC centrifugal pump is a simplified model of a centrifugal turbomachine. The original test case was presented by Combès [3] at a Turbomachinery Flow Prediction ERCOFTAC Workshop in 1999.

3.1 Geometry

The simplified model of the centrifugal pump has 7 impeller blades, 12 diffuser vanes and 6% vaneless radial gap as shown in Fig. 1. The geometric data and operating conditions are shown in Tab. 1. The test rig was built by M.Ubaldi et al.[4]. The purpose was to study the flow unsteadiness generated by rotor-stator interaction in a turbomachine.

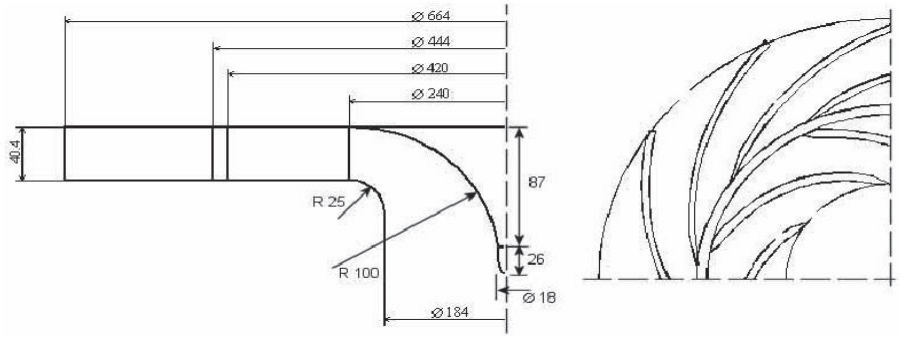

Fig. 1: Impeller and vaned diffuser geometry (Image taken from Ubaldi et al. [4]).

Impeller		**Diffuser**		**Operating conditions**	
Leading edge diameter	$D_1 = 240mm$	Leading edge diameter	$D_3 = 444mm$	Rotational speed	$n = 2000rpm$
Trailing edge diameter	$D_2 = 420mm$	Trailing edge diameter	$D_4 = 664mm$	Impeller tip speed	$U_2 = 43.98m/s$
Number of blades	$z_i = 7$	Number of vanes	$z_d = 12$	Flow rate coefficient	$\varphi = \frac{4Q}{U_2 \pi D_2^2} = 0.048$
Blade span	$z = 40.4mm$	Outlet diameter	$D_5 = 750mm$	Total pressure rise coefficient	$\psi = \frac{2(p_{out} - p_{in})}{8\rho U_2^2} = 0.65$
				Reynolds number	$Re = \frac{U_2 l}{\nu} = 6.5 * 10^5$
				Air density	$\rho = 1.2kg/m^3$

Tab. 1: Geometric data and operating conditions [4].

3.2 Measurements

The experimental data was provided by Ubaldi et al. [4]. The model operates in an open circuit with air directly discharged into the atmosphere from the radial diffuser. The pump operates at the nominal operating condition, at a constant rotational speed of 2000 rpm. (Reynolds number: 6.5×10^5, incompressible flow regime). Phase locked ensemble averaged velocity components have been measured with hot wire probes at the impeller outlet. The data includes the distribution of the ensemble averaged static pressure at the impeller front end, taken by means of miniature fast response transducers mounted at the stationary casing of the impeller. LDV measurements were also performed in the impeller and in the diffuser.
The measurements made by Ubaldi were made using a hot-wire probe at a radial distance 4 mm from the blade trailing edge (D_m/D_2=1.02). The results from the simulations were extracted in a similar way, as shown in Fig. 2.

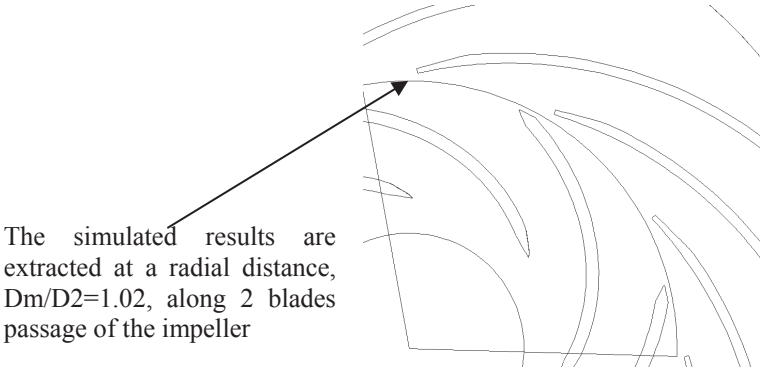

Fig. 2: Position of the hot-wire probe, and of the sampling of the simulated data.

3.3 Case-study set-up and cases

The ERCOFTAC centrifugal pump was used as a case study for the Fourth OpenFOAM Workshop, held in Montréal, Québec, in June 1-4 2009. It can be found in the turbomachinery Special Interest Group web page at the OpenFOAM Wiki (http://openfoamwiki.net/index.php/Sig_Turbomachinery), and in the OpenFOAM-extend SourceForge project (http://sourceforge.net/projects/openfoam-extend/). It includes block-structured meshes, scripts that automatically set up the cases, and automatic post-processing of the results and comparison with the measurements. There are also written descriptions of the OpenFOAM features that are used for the case-study.

In the present work, a 2D representation of the geometry is used. Previous simulations have been done by Bert, Combès and Kueny [5], who showed that relevant information could be recovered from 2D simulations although the real flow has 3D features. The 2D mesh was made using ICEM-HEXA, and the rotor and the impeller were meshed separately. The mesh is block-structured, and consists of about 94 000 cells, with an average Y+ value of 35.
The boundary conditions are shown in Tab. 2.

Calculated data for the 2D cases		**Boundary conditions**	
Inlet Diameter	D_0=200 mm	At the inlet	$V_{radial} = U_0$ $\frac{\mu_T}{\mu} = 10$ (viscosity ratio) $k = \frac{3}{2}U_0^2 I^2 = 0.48735 m^2/s^2$ (I=5%) $\varepsilon = \frac{C_\mu \rho k^2}{\mu_T} = \frac{C_\mu \rho k^2}{\mu(\mu_T/\mu)} = \frac{C_\mu k^2}{\nu(\mu_T/\mu)}$
Z thickness (OpenFOAM requires one cell thickness in 2D)	Z = 1mm		
Flow rate	$Q = \frac{\varphi U_2 \pi D_2^2}{4} = 0.292 m^3/s$		
Inlet radial speed	$U_0 = \frac{Q}{A_0} = \frac{Q}{2\pi r_0 z} = 11.4 m/s$	At the outlet	Average static pressure 0

Tab. 2: Computational parameters for the 2D cases.

The ERCOFTAC centrifugal pump (ECP) cases that are currently available are listed here:

- Steady state frozen rotor cases, using MRF (Multiple Reference Frames)
  - *ECPGgi2D*: The frozen rotor approach, and the GGI between the impeller and the diffuser.
  - *ECPStitchMesh2D*: The frozen rotor approach, where the rotor and stator meshes have been stitched together at the interface, forming a single mesh with hanging nodes at the interface.
- Unsteady sliding grid cases
  - *ECPMixerGgiFvMesh2D*: The sliding grid approach, where the GGI is applied between the impeller and the diffuser at each time step.
  - *ECPMixerFvMesh2D*: The sliding grid approach, where the rotor and stator meshes are stitched together at the interface at each time step, forming a single mesh with hanging nodes at the interface at each time step.

3.4 Results

3.4.1 Steady-state simulation – frozen rotor

The simulation was stopped after 5000 iterations, since all the residuals were below 10^{-5}. The frozen rotor approach gives something that resembles a snapshot of the real flow in the pump, but the advection of the impeller wakes in the diffuser region will by definition not be physical (see Fig. 3).

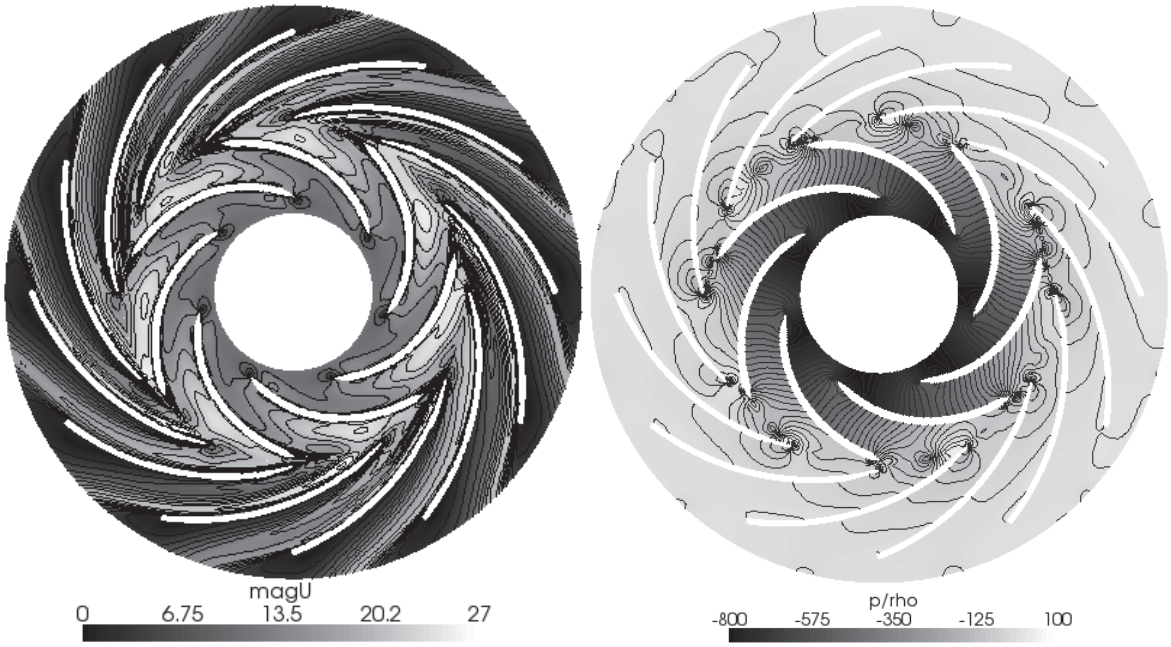

Fig. 3: Velocity magnitude and static pressure for the pump, for the frozen rotor simulation.

The computed velocities show some similarity with the experimental data, as shown in Fig. 4, however, the results do not agree perfectly with the experimental ones. Most of these differences are likely due to the frozen rotor formulation rather than the OpenFOAM implementation. A comparison with preliminary results from a commercial CFD code [6] shows that OpenFOAM gives similar results as commercial CFD codes for frozen rotor simulations.

The GGI and the stitched cases give exactly the same results as can be seen in Fig. 4, and it can thus be concluded that the interface coupling works as it should.

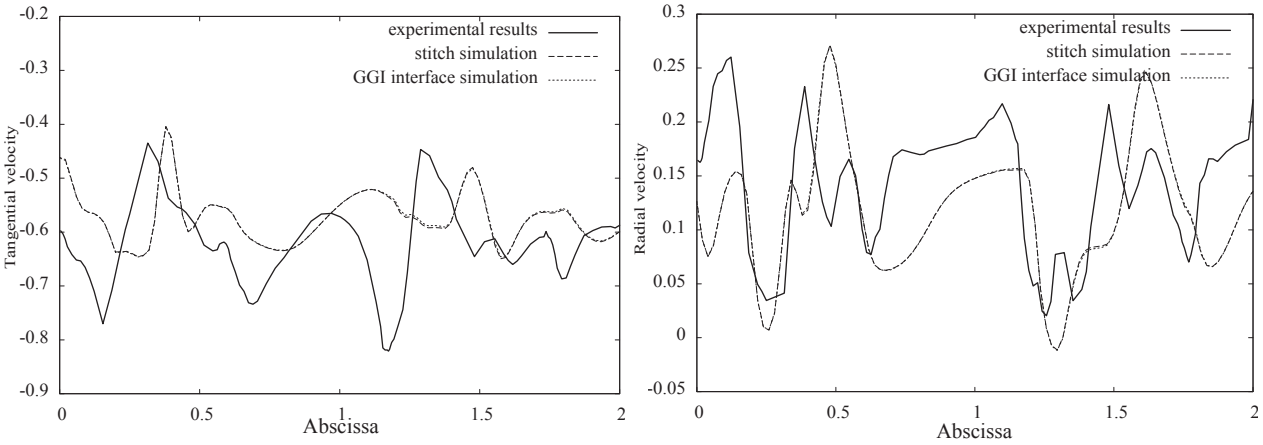

Fig. 4: Distributions of the tangential and radial velocities, for the two frozen rotor simulations compared to the experimental data. The two simulation results are identical.

3.4.2 Unsteady simulation, using the sliding grid approach

Both computations (*ECPMixerGgiFvMesh2D* and *ECPMixerFvMesh2D*) give the same results. Therefore, only the GGI approach will be discussed here.

With the unsteady simulation, the wakes are more visible, and they are advected properly between the diffuser blades, as shown in Fig. 5. There is a better, although not perfect, agreement between the simulations and the experimental data, compare to the frozen rotor simulation, see Fig. 6. However, the tangential velocity is slightly over-predicted.

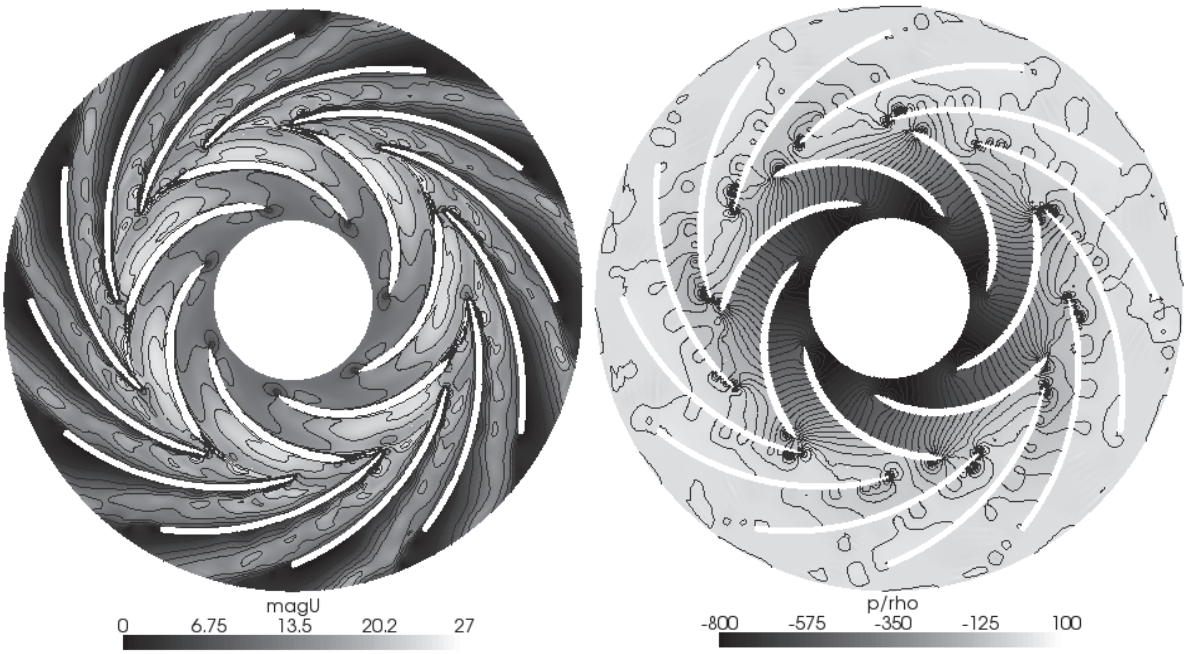

Fig. 5: Velocity magnitude and static pressure for the ERCOFTAC centrifugal pump, for the unsteady simulation

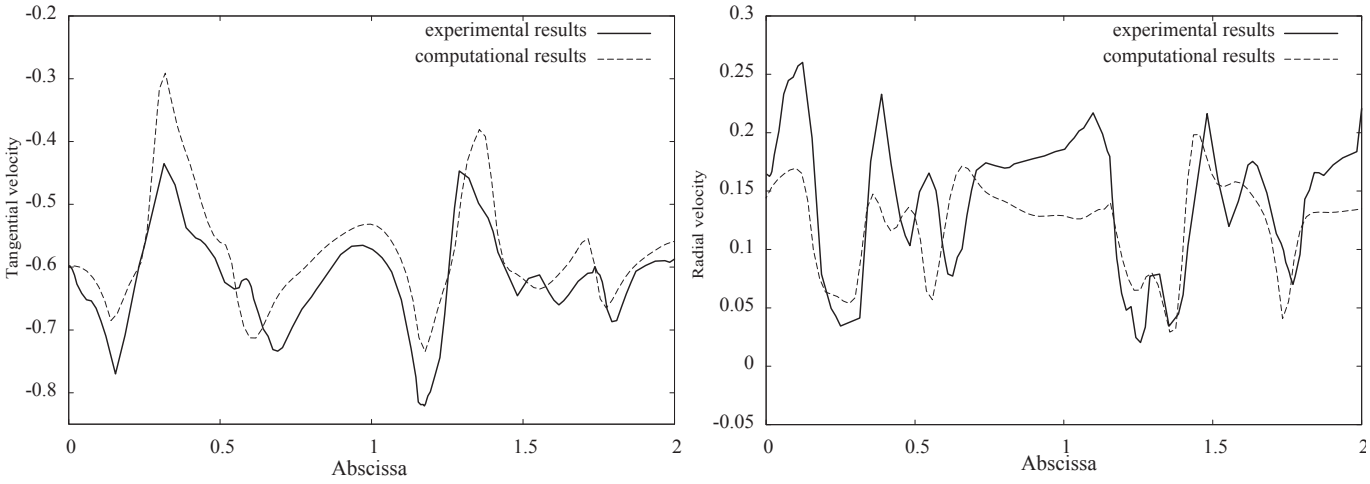

Fig. 6: Distributions of tangential and relative velocity for the unsteady simulation, compared to the experimental data.

4 IMPLEMENTATION DETAILS

4.1 Steady-state solver for Multiple Reference Frames

The solver used for the frozen rotor simulations, based on the Multiple Reference Frame (MRF) approach is named MRFSimpleFoam. It is a steady state solver for incompressible turbulent flow, using the SIMPLE algorithm for pressure-velocity coupling. The MRF approach implies that there is no relative mesh motion of the rotating and stationary parts. In a rotating reference frame, where the relative velocity is computed, the momentum equations must be modified with Coriolis and centrifugal terms. In the MRF approach, the momentum equations uses a mix of inertial and relative velocities, and only one extra term appears in the equations. Tab. 3 summarizes the formulation of the Reynolds Averaged Navier-Stokes equations in the inertial and the rotating frames, and the third alternative is what is implemented in MRFSimpleFoam.

Frame	Convected velocity	Steady incompressible Navier-Stokes equations
Inertial	Absolute velocity	$\begin{cases} \nabla \cdot (\vec{u}_I \otimes \vec{u}_I) = -\nabla(p/\rho) + \nu \nabla \cdot \nabla(\vec{u}_I) \\ \nabla \cdot \vec{u}_I = 0 \end{cases}$
Rotating	Relative velocity	$\begin{cases} \nabla \cdot (\vec{u}_R \otimes \vec{u}_R) + 2\vec{\Omega} \times \vec{u}_R + \vec{\Omega} \times \vec{\Omega} \times \vec{r} = -\nabla(p/\rho) + \nu \nabla \cdot \nabla(\vec{u}_R) \\ \nabla \cdot \vec{u}_R = 0 \end{cases}$
Rotating	Absolute velocity	$\begin{cases} \nabla \cdot (\vec{u}_R \otimes \vec{u}_I) + \vec{\Omega} \times \vec{u}_I = -\nabla(p/\rho) + \nu \nabla \cdot \nabla(\vec{u}_I) \\ \nabla \cdot \vec{u}_I = 0 \end{cases}$

Tab. 3: Summary of the Navier-Stokes equations for steady flow in multiple reference frames.

4.1.1 Frozen rotor

In the frozen rotor formulation, the rotating and stationary parts are considered to be at a fixed position relative to each other. The coupling between the rotor and stator domains are still resolved 360˚, but fixed in time. Since the rotor and the stator parts have been meshed separately, a connection must be made between these meshes. Two methods can be used for that in OpenFOAM. The first one is based on the topological changes technology (see section 4.3). The second method is the GGI (see section 4.4).

4.1.2 Mixing plane

Another solution to model the interface between the rotating and stationary parts is the mixing plane. At the interface the flow properties are circumferentially averaged. This will of course remove all transient rotor-stator interactions, but it still gives fairly representative results. A mixing-plane simulation only requires one rotor blade and one stator blade per stage, which significantly accelerates the solution procedure.
The mixing plane is under implementation in OpenFOAM at the moment, but there should be an implementation available in the coming year.

4.2 Unsteady solver for sliding grid

The solver used for the sliding grid simulations in this work is named turbDyMFoam. This is a solver for incompressible RANS simulations using the PISO algorithm for pressure-velocity coupling. The solver also uses libraries for mesh motion and deformation of polyhedral meshes [7], of which one of them handles partly rotating meshes. In the simulations the physical motion of the mesh is directly addressed. The coupling between the rotating and non-rotating parts of the mesh can be accomplished by either topological changes (see section 4.3) or GGI (see section 4.4).

4.3 Topological changes

Two parts of a mesh with coinciding faces can be attached to each other by connecting the faces of both parts. If the resulting mesh would not be conformal, OpenFOAM allows polyhedral cells, and may thus cut the faces to make the mesh conformal with hanging nodes. The sliding interface with topological changes in OpenFOAM uses this functionality at each time step, and deals with the topological changes associated to it. The topological modifier attach-detach is then used, and the rotating part of the mesh is detached from the static part. The rotation then occurs, and the mesh is attached again, as explained in Fig. 7. The black points show the vertices of a 2D cell, and it is shown that a non-conformal connection gives control volumes with hanging nodes.

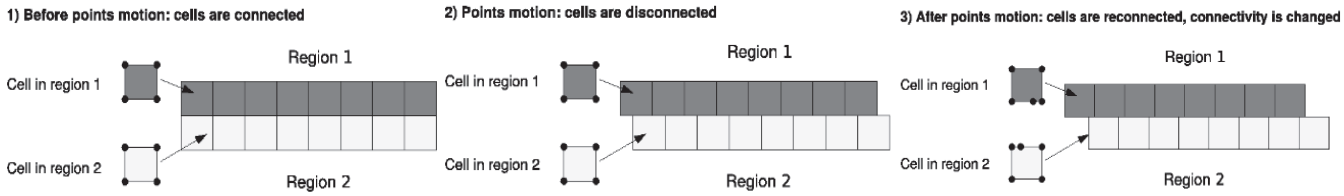

Fig. 7: Operation of a sliding interface, pictures from [7].

This operation can be quite time-consuming, as it needs to re-organize the topology and the internal numbering of faces and cells at each time step. However, the method is fully conservative.

4.4 General Grid Interface (GGI)

The GGI can be used to speed up the operation of the coupling between the rotor and stator domains. With the GGI, the modus operandi is quite similar as for the topological change method. The neighbours still need to be evaluated, but the attach-detach topological modifier doesn't need to be called anymore. This is a gain of time at each time step that is very noticeable on the whole simulation.
Implicit couplings are present in OpenFOAM in order to join multiple mesh regions into a single contiguous domain. But most of them are built to join conformal mesh regions, where

the patches nodes on each side of the interface are matching one to one. The GGI, developed by M. Beaudoin and H. Jasak [8] is a coupling interface used to join multiple non-conformal regions where the patches nodes on each side of the interface do not match.
A GGI is commonly used in turbomachinery, where the flow is simulated through a succession of various complex geometries. The requirement to fit all meshes with conformal matching interface is often very hard to reach. Using the GGI, non-conformal meshes can be designed separately, and joined together using one of many GGI alternatives.
The basic GGI is using weighted interpolation to evaluate and transmit flow values across a pair of conformal or non-conformal coupled patches. It is similar to the static sliding interface, although much simpler in the sense that no re-meshing is required for the neighbouring cells of the interface. The GGI weighting factors are basically the percentage of surface intersection between two overlapping faces.
The GGI implementation is using the Sutherland-Hodgman algorithm to compute the master and shadow face intersection surface area [9]. This algorithm is simple, fast and robust; being re-entrant, it allows for a very compact source code implementation. The Sutherland-Hodgman algorithm is also generic enough to handle any convex n-sided polygons.

5 Conclusions

The rotor-stator interaction features of OpenFOAM have been investigated and compared with experimental data of the ERCOFTAC centrifugal pump with a vaned diffuser. Both steady state simulations using Multiple Reference Frames and unsteady simulations using a transient solver with sliding mesh were performed. Good agreements were found with the experiments, but improvements can be made. The unsteady simulation showed a good behavior of the wakes being advected through the diffuser. It can be concluded that all the functionality is available in OpenFOAM for accurate rotor-stator analysis.
In order to improve the numerical results the same simulations will be performed in 3D, and alternative boundary conditions will be investigated. The coming mixing plane implementation will also be evaluated in the same case, and a tutorial on how to use the mixing plane will be released to the OpenFOAM community.

6 ACKNOWLEDGEMENTS

We would like to express our greatest acknowledgements to M. Ubaldi who made the experimental results of the ERCOFTAC centrifugal pump available, to share with the OpenFOAM community. We would also like to acknowledge OpenCFD Ltd, as well as Hrovje Jasak from Wikki Ltd, who distribute OpenFOAM, and helped us a lot to create this case study. We are very grateful to Hydro-Québec for its financial support and its participation in this project. Olivier Petit and Håkan Nilsson are partly financed by SVC (the Swedish Water Power Center, www.svc.nu). SVC has been established by the Swedish Energy Agency, ELFORSK and Svenska Kraftnät together with Chalmers University of Technology, Luleå University of Technology, Uppsala University and the Royal Institute of Technology.

7 REFERENCES

[1] Weller H.G, Tabor G, Jasak H, Fureby C., *"A tensorial approach to computational continuum mechanics using object-oriented techniques"*, Computers in Physics, Vol.12, No.6, 1998.

[2] Nilsson H., Page M., Beaudoin M., Gschaider B. and Jasak H., *"The OpenFOAM Turbomachinery Working Group, and Conclusions from the Turbomachinery Session of the Third OpenFOAM Workshop"*, 24th IAHR Symposium on Hydraulic Machinery and Systems, October 27-31, 2008, Foz Do Iguassu, Brazil.

[3] Combès, J.F., *"Test Case U3: Centrifugal Pump with a Vaned Diffuser"*, ERCOFTAC Seminar and Workshop on Turbomachinery Flow Prediction VII, Aussois, jan 4-7, 1999.

[4] Ubaldi M., Zunino P., Barigozzi G. and Cattanei A., *"An Experimental Investigation of Stator Induced Unsteadiness on Centrifugal Impeller Outflow",* Journal of Turbomachinery, vol.118, 41-54, 1996.

[5] Combès, J.F., Bert, P.F. and Kueny, J.L., *"Numerical Investigation of the Rotor-Stator Interaction in a Centrifugal Pump Using a Finite Element Method"*, Proceedings of the 1997 ASME Fluids Engineering Division Summer Meeting, FEDSM97-3454, 1997.

[6] Page, M., Théroux, E. and Trépanier, J.-Y., *"Unsteady rotor-stator analysis of a Francis turbine"*, 22nd IAHR Symposium on Hydraulic Machinery and Systems, June 29 – July 2, 2004, Stockholm, Sweden.

[7] Jasak, H., *"Dynamic Mesh Handling in OpenFOAM"*, 47th AIAA Aerospace Sciences Meeting Including the New Horizons Forum and Aerospace Exposition, 5-8 January, Orlando, Florida, 2008 (AIAA 2009-341).

[8] Beaudoin M. and Jasak H., *"Development of a Generalized Grid Interface for Turbomachinery simulations with OpenFOAM"*, Open Source CFD International Conference 2008.

[9] Sutherland I.E. and Hodgman G.W., *"Reentrant polygon clipping*", Communication of the ACM, vol.17, Number 1, 32-42, 1974.

Paper III

Comparison of Numerical and Experimental Results of the Flow in the U9 Kaplan Turbine Model (extended version to be submitted for IAHR 2010)

Olivier Petit, Håkan Nilsson

Division of Fluid Mechanics, Chalmers University of Technology,
Hörsalsvägen 7A, SE-41296 Göteborg, Sweden,
olivierp@chalmers.se, hani@chalmers.se

Abstract

The present work compares simulations made using the OpenFOAM CFD code with experimental measurements of the flow in the U9 Kaplan turbine model. Comparisons of the velocity profiles in the spiral casing and in the draft tube are presented. The U9 Kaplan turbine prototype located in Porjus and its model, located in Älvkarleby, Sweden, have curved inlet pipes that lead the flow to the spiral casing. Nowadays, this curved pipe and its effect on the flow in the turbine is not taken into account when numerical simulations are performed at design stage. To study the impact of the inlet pipe curvature on the flow in the turbine, and to get a better overview of the flow of the whole system, measurements were made on the 1:3.1 model of the U9 turbine. Measurements were taken at the inlet of the spiral casing and just before the guide vanes, using the laser Doppler anemometry (LDA) technique. In the draft tube, a number of velocity profiles were measured using the LDA techniques. The experimental results are used to specify the inlet boundary condition for the numerical simulations in the draft tube, and to validate the computational results in both the spiral casing and the draft tube.
The numerical simulations were realized using the standard k-ε model and a block-structured hexahedral wall function mesh.

Keywords: CFD, Water Turbine, Draft Tube, Spiral Casing, Distributor, OpenFOAM, Flow Measurements.

1. Introduction

Harvesting energy from the flow of water has been done for centuries, and it presents many advantages that makes it widely attractive. Hydro power generates nowadays more than 17 % of the total electricity needs in the world. One of the advantages of a hydro power plant compared to other types of plants is its longevity. Many of the existing dams have been operative for the last century, and it seems that they will continue to do so for many more decades. The power plant is of course closely monitored and its health is regularly checked, but if well-built, a dam can last for a long time. However, due to diverse issues, such as cavitation or vibration, parts of the turbine-generator units need to be replaced every decade or two. During this elapsed time, technology evolves, and so does the turbine design. It is the case for the Porjus hydraulic power plant located in the north of Sweden. Active since 1915, one of its units called U9 was replaced during the last decade. The main focus of the new U9 Kaplan turbine is to allow research on a real scale turbine, rather than production [1]. Few detailed measurements are made in water turbines. During design phase, overall quantities such as efficiency are usually measured, rather than detailed pressure and velocity profiles. The U9 prototype facilitates such detailed investigations. It is somewhat smaller than the previous unit, and a curved pipe was inserted into the old penstock when assembling the new prototype.

The use of computational fluid dynamics (CFD) in the design and refurbishment process is becoming increasingly popular due to its flexibility, its detailed flow description and cost-effectiveness compared to the model testing usually used in the development of turbines. However, to get a good description of the flow in such large systems, the appropriate simulation parameters need to be set. Hence many models in CFD are calibrated and validated through simpler geometries and flow patterns. Analytical results, as well as experimental databases are often used to compare and validate simulations. The aim of the U9 project is to create a database of pressure and velocity patterns that can be use to validate CFD simulations, and to investigate the impact of the curved pipe on the flow in the U9 turbine. The measurements are performed on a 1:3.1 scale Kaplan turbine model. The database is constituted of three different operative conditions: peak efficiency and two off-design points.

Accurate CFD results provide a good understanding of the flow in the turbine, and due to technological improvements, increase of RAM memory and CPU's speed for example, the whole water turbine can now be computed. However, studying such a system requires to do simulations on many computers, in parallel. This can become costly when commercial softwares are used. The alternative that was chosen in this work is OpenFOAM, which is an OpenSource CFD tool written in C++. Previous comparisons [2], [3], and [4] show that it is a competitive and high quality tool that gives similar results as commercial softwares.

This work presents comparisons between experimental and numerical results, in the U9 spiral casing and draft tube. In this work, the comparisons are limited to one working point, the best efficiency point (BEP), and limited to the velocity profiles.

2. Test rig and experimental setup

2.1. Test rig

The test rig used to do the measurements is located at the Vattenfall Research and Development (VRD) model test facility in Älvkarleby, Sweden. It is a closed loop system where the absolute pressure in the downstream tank can be regulated to control the presence of cavitations. It is a 1:3.1 scale model of the U9 prototype. The best efficiency point corresponds to a guide vane angle of 26 degrees, and a discharge of 0.71 m^3/s. An overview of the test rig is given in Fig. 1 where the curved inlet pipe is represented. The measurements used for the validation in the present work were made in the optical correction box, the spiral casing and the draft tube cone.

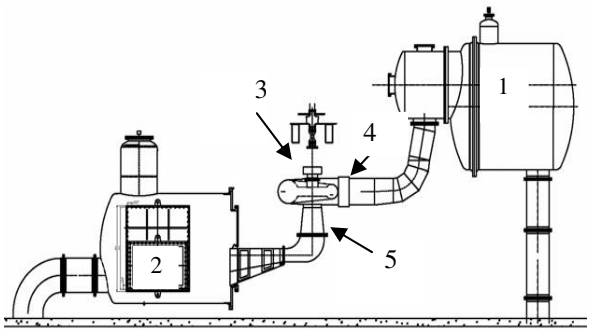

1. High pressure tank.
2. Low pressure tank.
3. Spiral Casing.
4. Optical correction box.
5. Draft tube cone.

Fig. 1: Test rig of the U9 Kaplan model [5].

2.2. Measurements in the U9 spiral casing

In order to investigate the effect of the curved inlet pipe on the flow, and to generate a database for future numerical simulations, measurements were made at the spiral casing inlet and in the spiral casing before the wicket gates. The measurements were presented by Mulu et al. [5].

The inlet of the U9 model spiral casing is a circular pipe with an inner radius of 316 mm. A plexiglas pipe 290 mm long was mounted between the inlet of the spiral casing and the curved pipe, see Fig. 2. To avoid refraction caused by the surface curvature of the inlet pipe, a square optical box, filled with index matching liquid is placed around the pipe [5]. LDA measurements were performed from both sides of the pipe, along five horizontal and one vertical axis, as shown in Fig. 2.

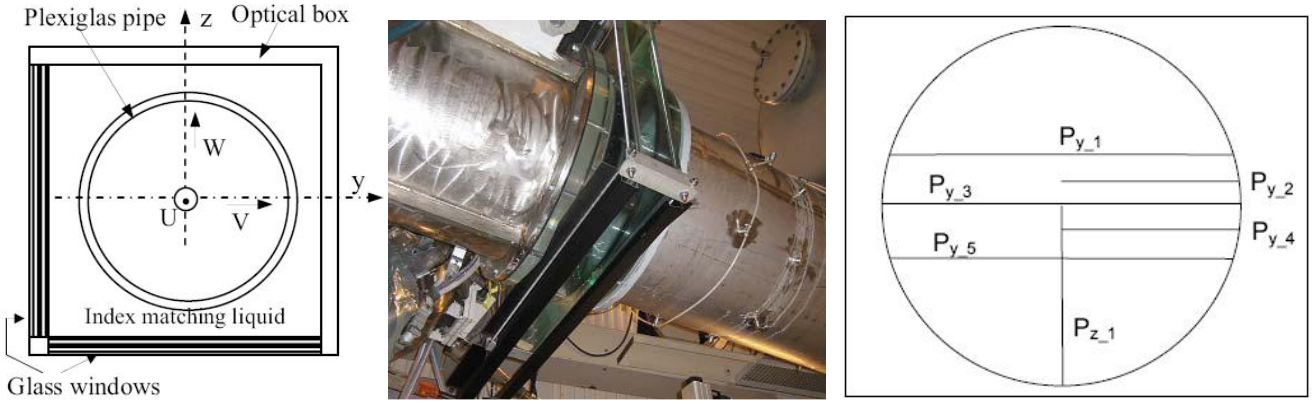

Fig. 2: Inlet section of the spiral casing (left, centre), and locations of the measured velocity profiles in the circular section [5].

In the spiral casing, two windows were installed in the lower side at the angular positions -56.25 degrees, (SI) and -236.25 degrees (SII) to perform LDA measurements, as shown in Fig. 3. The windows were placed at the centre of the casing, at a distance from the stay vanes. The LDA measurements were more accurate than at the inlet, as the windows are planar, and thus do not cause any refraction problem.

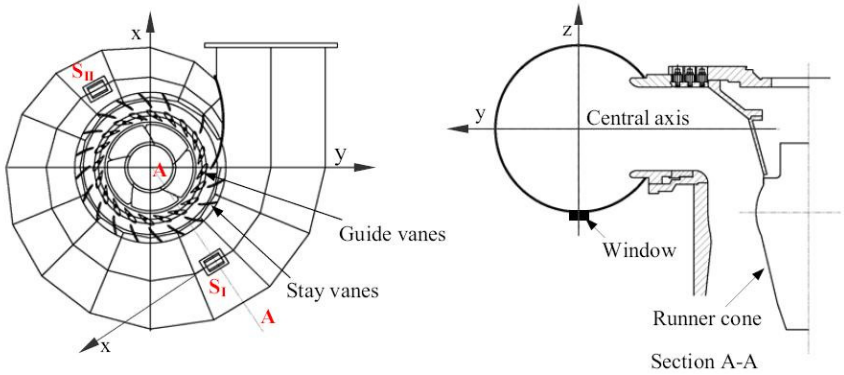

Fig. 3: Location of the windows in the spiral casing (left) and of the measurement axis z (right) [5].

2.3. Measurements in the U9 draft tube

The measurements of the velocity profiles in the draft tube were performed and presented by Mulu et al. [6], while pressure measurements were performed by Jonsson et al. [7]. The system used to measure the velocity profiles, both in the spiral casing and in the draft tube, is a two-component LDA system from Dantec with an 85 mm optical fibre probe and a front lens of 600 mm focal length. The measurements were performed at four different windows with angular positions (AP) of 0, 90, 180 and 270 degrees, as shown in Fig. 4. The axial and tangential velocity profiles were measured at profiles I, II and III (PI, PII, PIII) for the four different angular positions. The three profiles are located in the draft tube cone. Profile I is located below the runner, while Profile II and III are located respectively in the middle and close to the end of the cone [6].

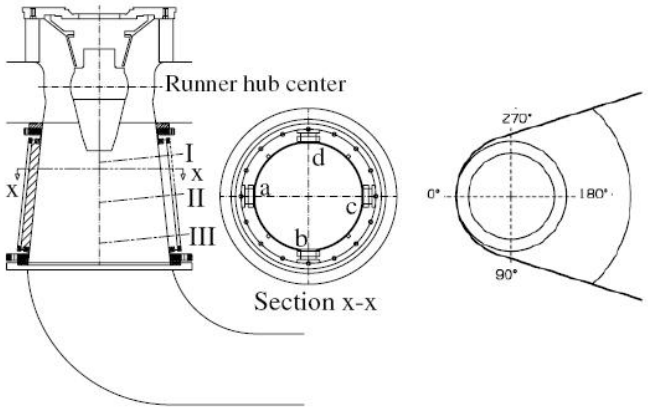

Fig. 4: Window locations at the draft tube cone: a is at 0°, b at 90 °, c at 180°, and d at 270°. I, II, and III are the three sections where the velocity profiles are measured in each window [6].

2.4. Operating conditions

The measurements have been carried out at three different loads, at best operating point of the turbine and at two off-design operating points (to the left and right of the propeller curve). The operational net head H=7.5 m, the runner blade angle β=0.8°, and a runner speed N=696.3 rpm were used throughout the entire period of measurements. The working guide vane angle and the volume flow rate of the three working conditions are summarized in Table. 1. The results presented in this paper are limited to the best efficiency point.

Operating point	Left	BEP	Right
Guide vane angle (α) in degree	20	26	32
Volume flow rate Q (m3/s)	0.62	0.71	0.76

Table. 1: Operational condition parameters [5].

3. Computational domain and OpenFOAM setup

3.1. Spiral casing computational domain and setup

The spiral casing computational domain starts with the high-pressure tank and includes the curved inlet pipe, the spiral casing as well as the wicket gate, see Fig. 5. The domain was realized in ICEM Hexa, and is divided in four different parts: the inlet tank, the inlet curved pipe, the spiral casing, and the wicket gate. Those four different parts are coupled in OpenFOAM using the General Grid Interface (GGI) developed by Beaudoin and Jasak [8]. The mesh is fully hexahedral, and consists of 5 million cells. The incompressible Reynolds-Averaged Navier-Stokes equations are solved, using the finite volume method and the standard k-ε

model closure. At the walls the log-law treatment is applied and the average y+ values range between 50-100. The boundary condition at the inlet is a plug flow with the nominal discharge 0.71 m^3/s. The turbulent kinetic energy is calculated so that the turbulent intensity is 10%, and the turbulence dissipation is chosen so that $\nu_T/\nu=10$. At the outlet, a mean pressure of 0 is set. A second-order upwind scheme is set for the convection, while the first-order upwind scheme is used for the turbulence parameters.

3.2. U9 draft tube computational domain and setup

The draft tube mesh is fully hexahedral, and consists of 1.1 million cells. The draft tube computational domain is shown in Fig. 6. Also in this case, the standard k-ε model is used with wall functions. The inlet boundary condition for velocity and turbulence is given by the measurements, see Fig. 7. Measurements of the axial and tangential velocity were realized by Mulu [6] along a horizontal cross-section, at a radius R=268.88 mm, i.e the same point on the shroud as section P1 but along a horizontal line,, for two different angular position 0 and 270°. The inlet boundary condition for the simulation in OpenFOAM is the average tangential and axial velocity of those two profiles. Because no radial velocity were measured, the radial velocity at the inlet is set to zero. The same numerical schemes have been used as for the spiral casing simulations.

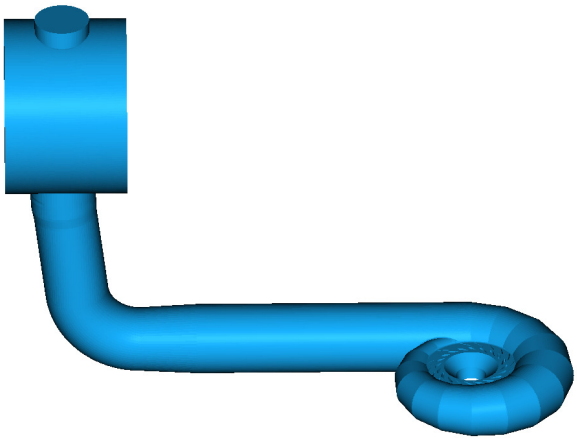

Fig. 5: Computational domain of the U9 spiral casing.

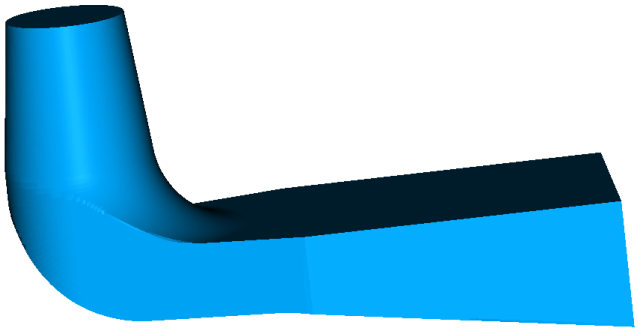

Fig. 6: Computational domain of the U9 draft tube.

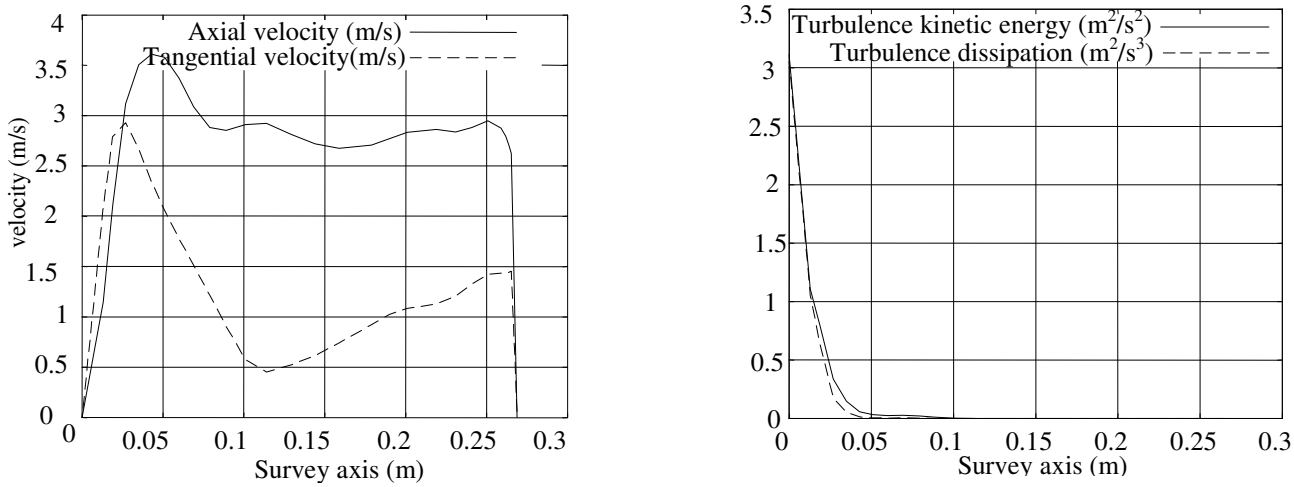

Fig. 7: Inlet boundary conditions used for the U9 draft tube.

4. Results

An overview of the flow in the spiral casing and draft tube is shown in Figs. 8, 9, 10 and 11. The importance of including the curved pipe in the computational domain is shown in Fig.8, and the recirculation is still visible at the inlet of the spiral casing, in Fig. 9. The accuracy of the recirculation prediction in the numerical results is strongly dependent on the choice of the turbulence model that is made, as well as the choice of boundary condition at the wall. Detached-eddy Simulation (DES) should predict the length of the detached boundary layer, and hence the recirculation, much better than the k-ε model. That will be done in future work.

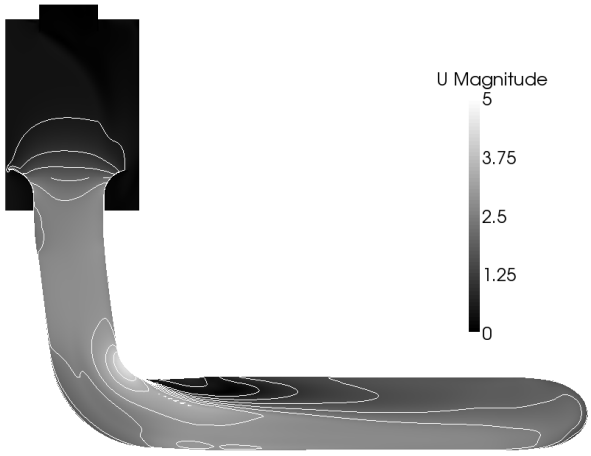

Fig. 8: Velocity magnitude in the inlet pipe.

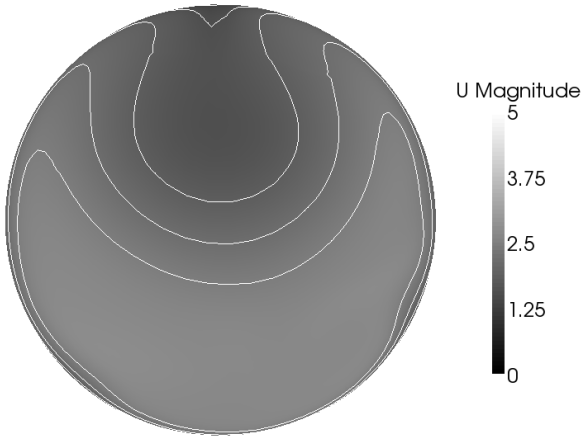

Fig.9: Velocity magnitude at the spiral casing inlet measurement section.

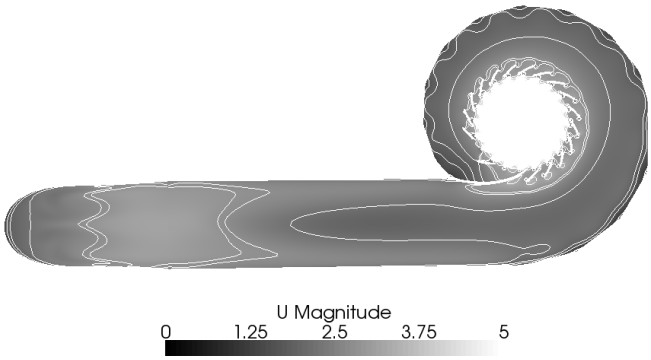

Fig. 10:Velocity magnitude in the spiral casing.

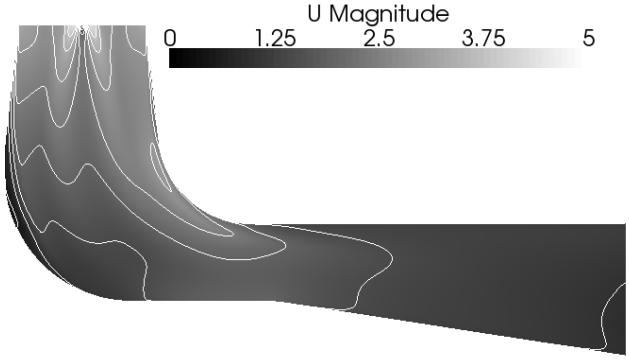

Fig.11: Velocity magnitude in the draft tube.

.

4.1. Results in the spiral casing

At the inlet of the spiral casing, the experimental axial velocity profiles at Py_1, Py_5 and Pz, specified in Fig. 2, are compared with the numerical results in Fig.12. The analysed data are presented in dimensionless form using, R_{inlet}=0.316m, and $v_{Bulk} = \frac{Q}{\pi * R_{inlet}^2}$, Q=0.71 m.s^{-1}. The flow predicted by OpenFOAM shows a similar behaviour as the measured flow. The axial velocity at Py_1 is lower than that at profile Py_5. The M-shape character in the velocity distribution is due to the pair of counterrotating Dean vortices, which is known in a circular bend flow. Since the axial velocity distribution is not uniform in the plane due to lower velocity close to the upper wall, fluid particles with higher velocity are forced to move to the outer side, and those with lower velocity to the centre. This is due to the curvature which causes a positive gradient of the centrifugal force from the centre to the outer wall. This force and the presence of a boundary layer at the wall due to the fluid adhesion to the wall combined are responsible for this kind of flow behaviour [5].

The difference between the prediction of OpenFOAM and the measured flow can be explained by accuracy issues. The refraction of the cylindrical pipe creates a small error in the measurements, especially close to the wall. Moreover, the simulations done with OpenFOAM use a basic k-ε model that does not fully predict the flow especially close to the wall, and in the recirculation region after the bend, shown in Fig. 8. At profile P_z, which is at the center line of the pipe, the numerical results show good agreement with the experimental values.

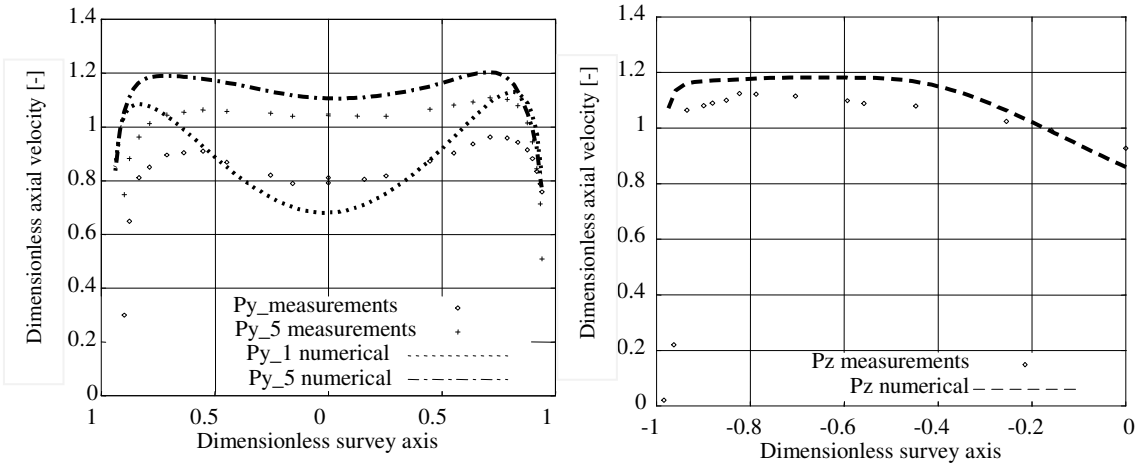

Fig.12: Axial velocity profiles at profile Py_1 and Py_5 (left), and Pz (right).

The comparison inside the spiral casing is done at the two positions (SI and SII) described in Fig. 3. Axial and tangential velocity profiles are shown in Fig.13. The reference point is located at the lower wall of the spiral casing.

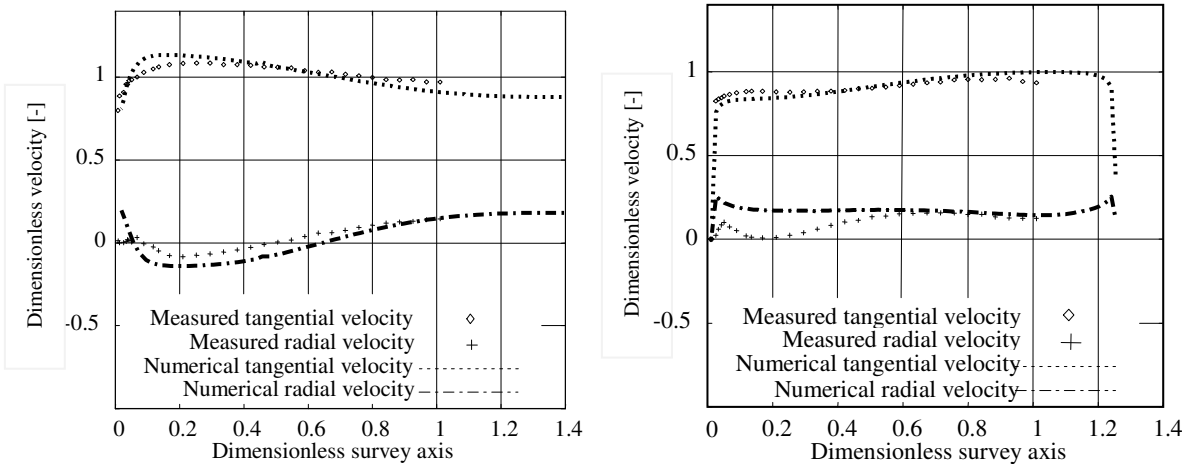

Fig.13: Dimensionless radial and tangential velocity at SI (left) and SII (right), inside the spiral casing.

In this comparison, the radial velocity is defined as positive toward the centre. The radial velocity measured at location SI shows the presence of a secondary flow yielding negative radial velocities. This secondary flow is not observed at location SII. The numerical prediction of the flow inside the spiral casing is accurate, though it tends to yield a slighlty different radial velocity distribution than the experimental measurements at Section I.

4.2. Results in the draft tube

In the draft tube, comparisons of the numerically predicted flow and the measurements are made in two different windows, a and c (see Fig. 4). The results are presented in Fig.14. The reference point for this comparison is at the centreline of the draft tube, and the survey axis is normalized by the radius of the runner, R_{Runner}=0.5m. Close to the inlet of the draft tube, the predicted flow is similar to the measured flow. However, the difference at the centre of the draft tube is already visible. The numerical simulation does not predict the flow features very well in the draft tube, and the more downstream it goes, the less accurate the results become. The reason to this unaccuracy is the inlet boundary condition. The velocity profile set at the inlet of the draft tube is an average value of the flow measured at window a and d at section SI. That means that we set a symmetric swirling flow at the inlet. In reality, the swirl flow is asymmetric as wakes are coming down from the runner. Moreover, the real profiles at windows a, b, c and d differ significantly which is here neglected. It is further questionable to specify a steady axi-symmetric inlet boundary condition in a region of high unsteadiness and non-axi-symmetry. Finally, it was shown at the Turbine-99 workshop [9] that ignoring the radial velocity profile when setting the inlet boundary condition leads to a wrong prediction of the flow in the draft tube. In the present work, the inlet boundary condition was taken from 2D LDA measurements, and radial velocity measurements were not available. Close to the wall, however, the flow is rather well predicted, both for the elbow window (window c) and for the window a. This is promissing, and a more precise inlet boundary condition should result in an accurate prediction of the flow. However, for accurate results, the runner must be included in the simulation. That will be done in future work.

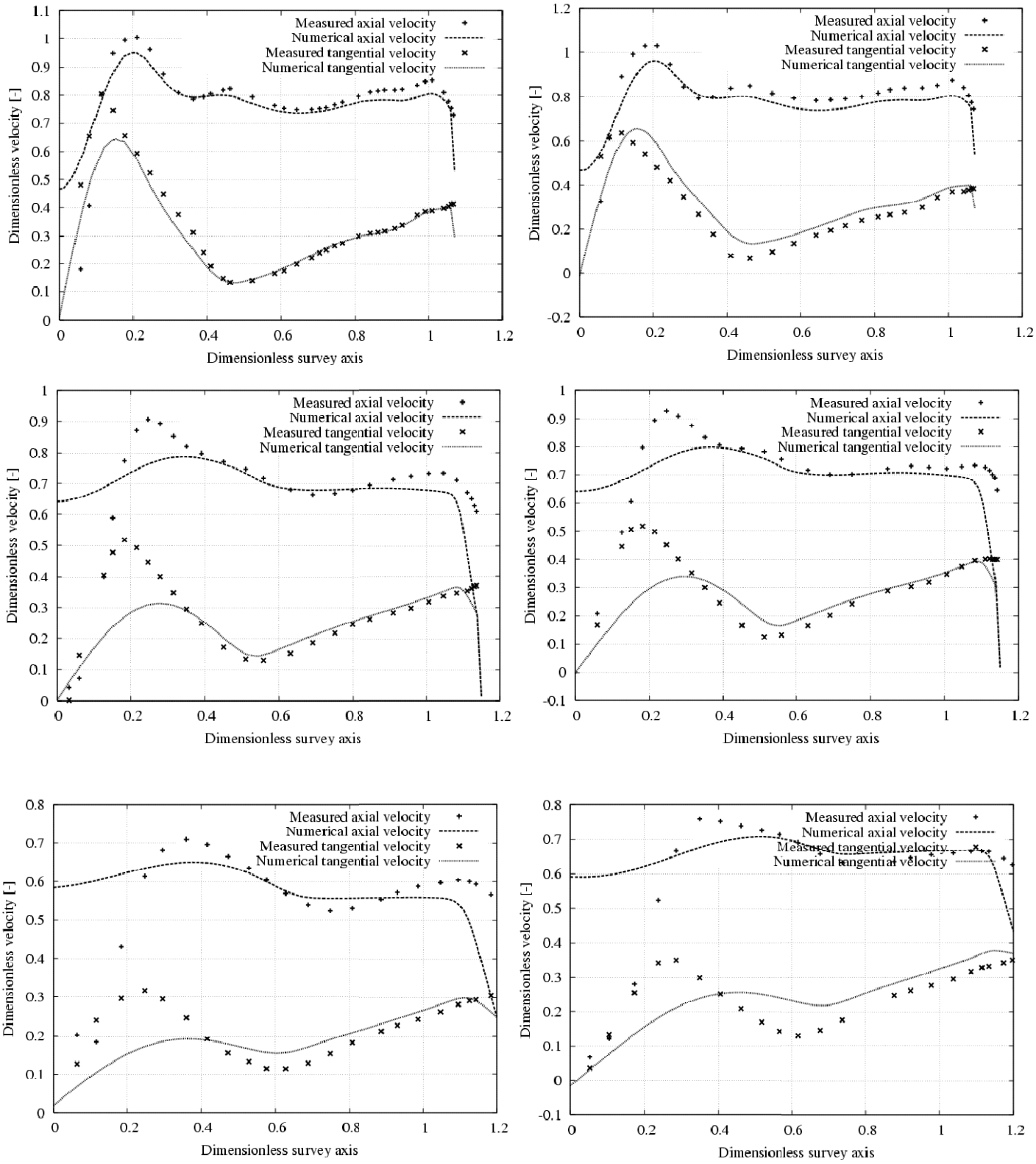

Fig.14: Velocity profiles for windows a (left) and c (right), at three different sections: from top to down, SI, SII and SIII.

5. Conclusion

Comparisons between numerical simulations and experimental results in the U9 spiral casing and draft tube have been presented. The results show the importance of setting appropriate boundary conditions when numerically trying to predict the flow in water turbines.

In the spiral casing, the comparison shows the effect a curved pipe has on the spiral casing inlet flow. In the draft-tube, the importance of defining an appropriate inlet boundary condition is the key to succesfully predict the flow features of the draft tube. However, to predict the flow as accurately as possible, it is important to couple the runner with the draft tube, and to compute unsteady simulation.

The numerical simulations predict the overall flow features in the spiral casing and in the draft tube rather well. The predicted flow is similar to the measured flow, and this work sets the base for future investigations. Future work in the U9 project is the investigation of more accurate turbulence models in the spiral casing, in order to accurately predict the turbulent flow features. In the draft tube, an estimation of the radial velocity should get a better flow prediction. Ultimately, unsteady simulations of the U9 Kaplan turbine coupled with the draft tube using a sliding grid should predict a very accurate flow.

6. Acknowledgement

The research presented in this work was carried out as a part of the Swedish Hydropower Centre (SVC). SVC has been established by the Swedish Energy Agency, Elforsk and Svenska Kraftnät together with Luleå University of Technology, The Royal Institute of Technology, Chalmers University of Technology and Uppsala University. www.svc.nu.

The authors would like to thank the staff at Vattenfall Research and Development for the help and support during the measurements, and the Swedish National Infrastructure for Computing (SNIC) and Chalmers Centre for Computational Science and Engineering (C^3SE) for providing computational resources. The U9 turbine geometry was shared by Andritz, and their collaboration and help is gratefully ackowledged.

7. References

[1] Cervantes, M.J., Jansson, I, Jourak, A., Glavatskikh, G. and Aidanpää, J.O., 2008, "Porjus U9, A Full-Scale Hydropower Research Facility", in Proceedings of the 24th IAHR Symposium on Hydraulic Machinery and Systems, Foz Do Iguassu, Brazil.

[2] Petit, O., Nilsson, H., Vu, T., Manole, O., and Leonsson, S., 2008, "The Flow in the U9 Kaplan Turbine - Preliminary and Planned Simulations Using CFX and OpenFOAM", in Proceedings of the 24th IAHR Symposium on Hydraulic Machinery and Systems, Foz de Iguassu, Brazil.

[3] Nilsson, H., and Page, M., 2005, "OpenFOAM simulation of the flow in the Hölleforsen draft tube model", in Proceedings of the 3rd IAHR/ERCOFTAC Workshop on draft tube flows, Porjus, Sweden.

[4] Muntean, S., Nilsson, H., and Susan-Resiga, R., 2009, "3D Numerical Analysis of the Unsteady Turbulent Swirling Flow in a Conical Diffuser Using Fluent and OpenFOAM", 3rd IAHR International Meetings of the Workshop on Cavitation and Dynamic Problems in Hydraulic Machinery and Systems, C4, Brno, Czech Republic.

[5] Mulu, B., 2009, "Experimental and Numerical Investigation of Axial Turbine Models", Licenciate Thesis, Luleå University of technology, Sweden.

[6] Mulu, B., and Cervantes, M., 2009, "Experimental Investigation of a Kaplan Model with LDA", 33rd IAHR Congress Water Engineering for a Sustainable Environment.

[7] Jonsson, P., and Cervantes, M, "Time Resolved Pressure Measurements on a Kaplan Model."

[8] Beaudoin, M., and Jasak, H., 2008. "Development of a Generalized Grid Interface for Turbomachinery simulations with OpenFOAM", OpenSource CFD International Conference , Berlin, Germany.

[9] Cervantes, M., Gustavsson, L., Page, M., ans Engström, F., 2006, "Turbine-99, a summary", 23rd IAHR Symposium, Yokohama.

Paper IV

A Swirl Generator Case Study for OpenFOAM (extended version to be submitted for IAHR 2010)

Olivier Petit[1], Alin I. Bosioc[2], Håkan Nilsson[1], Sebastian Muntean[3], Romeo F.Susan-Resiga[2]

[1]Division of Fluid Mechanics, Chalmers University of Technology
Hörsalsvägen 7A, SE-41296 Göteborg, Sweden
E-mail: olivierp@chalmers.se, hani@chalmers.se
[2]Department of Hydraulic Machinery, "Politehnica" University of Timisoara
Bv. Mihai Viteaazu 1, Timisoara 300222, Romania
E-mail: alin@mh.mec.upt.ro, resiga@mh.mec.upt.ro
[3] Centre of Advanced Research in Engineering Sciences, Romanian Academy – Timişoara Branch
Bv. Mihai Viteazu 24, RO-300223, Timişoara, Romania
E-mail: seby@acad-tim.tm.edu.ro

Abstract

This work presents numerical results, using OpenFOAM, of the flow in the swirl flow generator test rig developed at Politehnica University of Timisoara, Romania. The work shows results computed by solving the unsteady Reynolds Averaged Navier Stokes equations. The unsteady method couples the rotating and stationary parts using a sliding grid interface based on a GGI formulation. Turbulence is modeled using the standard k-ε model, and block structured wall function ICEM-Hexa meshes are used. The numerical results are validated against experimental LDV results, and against designed velocity profiles. The investigation shows that OpenFOAM gives results that are comparable to the experimental and designed profiles. This case study was presented at the 5th OpenFOAM Workshop, held in Gothenburg, Sweden, as a tutorial on how to treat turbomachinery applications in OpenFOAM.

Keywords: Swirl generator, OpenFOAM, CFD, Validation, Runner, Draft tube, Rotor-Stator Interaction.

1. Introduction

Nowadays, due to the variable demand of the energy market and new intermittent energy sources, a new parameter is often important for water power: flexibility. Water turbines now operate over an extended range of regimes that can be quite far from the best efficiency point. The runner is designed so that the swirl generated by the guide vanes is more or less neutralized at the best efficiency point. However, at part load operation (away from the efficiency point), a strong swirling flow exits the runner. This is called a vortex rope. This phenomenon leads to large periodic pressure fluctuations that increase the risk of fatigue.

The importance of predicting such phenomena has lead to many studies. One of those is the Flow Investigation in Draft Tubes (FLINDT) research project [1]. The main objective of the FLINDT project was to investigate such phenomena and to provide an extensive database for a range of different operating points. Such experimental projects are usually complex and measurements are performed on reduced scale models. The team at the Politehnica University of Timisoara (UPT), National Centre for Engineering Systems with Complex Fluids (NCESCF) has developed such a simplified swirl generator to further study the precessing vortex rope [2]. The swirl generator was designed to give a swirl profile similar to that in the FLINDT project. The test rig was developed and manufactured in order to provide a good visualization of the phenomenon, as well as to investigate the velocity field of the swirling flow [3, 4]. The stay vanes and runner blades were designed using the inverse design methodology [15] in order to create a precessing vortex rope [5]. One of the purposes of this test rig is to investigate the viability of reducing pressure fluctuation of a precessing vortex rope by axial jet control in the discharge cone. This novel technique was introduced by Susan-Resiga et al. [6] to control the draft tube instability at partial discharge. Measurements on the test rig showed that a 10% jet discharge gives a maximum pressure recovery and creates no pressure fluctuations [7]. This conclusion was asserted by 3D unsteady numerical investigation using Fluent of the swirling flow using jet control [8]. It is nonetheless not acceptable to bypass the runner with such a large fraction of the turbine discharge. However, Susan-Resiga et al. [9] have also developed a flow feedback approach for the jet, that supplies the jet without any additional losses in the turbine.

The simple geometry of the test rig, as well as the quality of the measurements done by Bosioc et al. [10] makes this a very good case study for turbomachinery applications in OpenFOAM. OpenFOAM is an object oriented OpenSource library written in C++. With regards to basic features, such as turbulence models and discretization schemes, OpenFOAM is a competitive and high quality tool that

is constantly evolving. Preliminary simulations were realized on the conical diffuser of the test rig [11], which showed that OpenFOAM gives as accurate results as commercial software.

The community driven OpenFOAM Turbomachinery Working Group [12] develops and validates OpenFOAM for turbomachinery applications. The swirling flow generator was chosen as a case study for the 5th OpenFOAM workshop held in Gothenburg, Sweden, and comparison between numerical results and measurements were presented. The goal of the Turbomachinery Working Group is to release this case study so that anyone who would like to learn OpenFOAM, or become more familiar with turbomachinery features in OpenFOAM, can learn how to set up, compute and analyse such problems.

2. Experimental setup

A cross-section of the test rig is presented in Fig. 1. The original test case was presented by Bosioc et al. [10] and was developed at Politehnica University of Timisoara. The swirling flow apparatus consists of four leaned strouts, 13 guide vanes, a free runner with 10 blades and a convergent divergent draft tube [3-5]. The guide vanes create a tangential velocity component, while keeping practically a constant pressure . The purpose of the free runner is to re-distribute the total pressure by inducing an excess in the axial velocity near the shroud and a corresponding deficit near the hub, like Francis turbine operation at 70% partial discharge. The runner blades act like a turbine near the hub, and a pump near the shroud. Thus the runner spins freely, without any total torque.

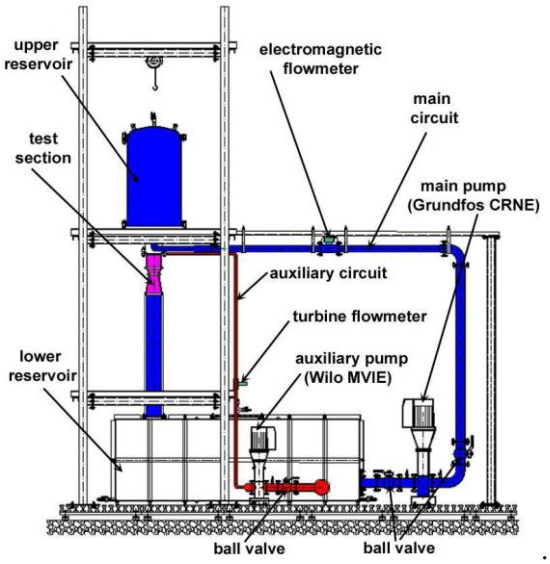

Fig. 1: Closed loop test rig for experimental investigations of swirling flow.

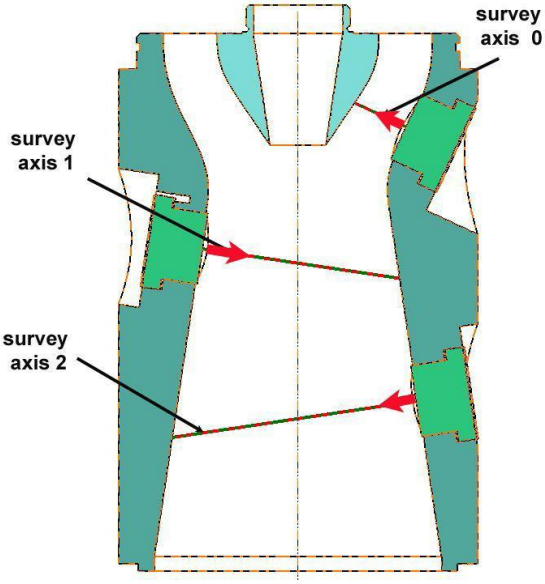

Fig. 2: Survey axes for LDV measurements

The test rig consists in a main circuit, used to supply the swirling flow section, and an auxiliary circuit that is used when tests are performed using axial jet control (see Fig. 1). The main centrifugal pump that provides the flow has a variable speed delivering 0-35 l/s. The swirling flow test section is made of plexiglass, so that visual observation is possible and to facilitate optical measurements. The measurements were realized at Politehnica University of Timisoara and were first presented by Bosioc et al. (10). The experimental data was measured with help of two-component Laser-Doppler Velocimetry (LDV). 10 μm aluminum particles were used to reflect the laser beam. The velocity measurements were realized in three different optical windows, the first located in the convergent part of the simplified draft tube, and the other two located in the axi-symmetric diffuser (see Fig. 2). The reference for the survey axis is set at the wall, as shown by the arrows in Fig. 2. On survey axis 0, 31 points were measured, while survey axis 1 contains 113 points, and survey axis 2 contains 141 points. The flow rate was kept at 80% of the maximum power of the pump, that is 30 l/s. The rotational speed of the free runner was 870 rpm. In order to get a time-averaged velocity profile, each point was sampled for a period of 25 seconds (5000 samples). Dimensionless form was used in the analysis of the velocity profiles, normalizing the abscissa by R_{Throat}=0.05m, and the velocity profiles by $v_{Throat} = \frac{Q}{\pi . R_{Throat}^2}$,Q=30 l/s.

For clarity, in the following discussion, the first survey axis is called **W0,** the second survey axis is called **W1** and the third one **W2**.

3. Computational domains and OpenFOAM numerical set-up

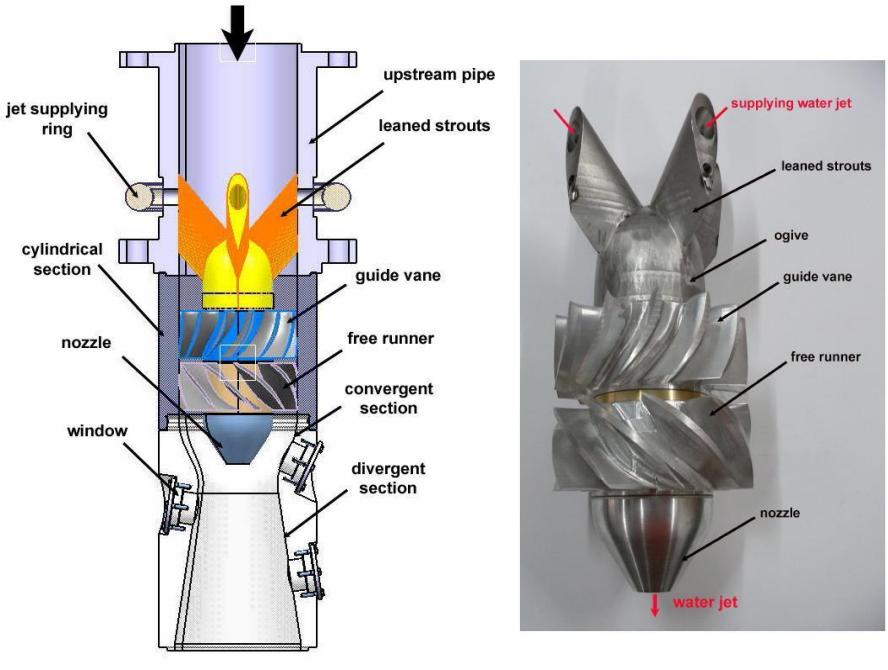

Fig. 3: Meridional cross-section of the swirling flow apparatus.

The computational domain consists of the whole test rig shown in Fig. 3. The mesh was generated in ICEM-Hexa, and consists of four different parts (see Fig. 4): the leaned strouts, the guide vanes, the free runner and the draft tube. The four different parts are coupled in OpenFOAM using the General Grid Interface (GGI), developed by Beaudoin and Jasak [13]. The mesh is fully hexahedral, and consists of 2.8 million cells. The incompressible unsteady Reynolds-Averaged Navier-Stokes equations are solved, using the finite volume method and the standard k-ε turbulence model. At the walls, the log-law treatment is applied, and the average y+ values range between 50-200. The boundary condition at the inlet is a plug-flow with the nominal discharge 30 l/s. The turbulence kinetic energy is set to 0.1, and the dissipation to 90, so that the turbulence intensity is of the order of 10% and the viscosity ratio ν_T/ν=10. The velocity and turbulence equations use the homogeneous Neumann boundary condition at the outlet. The pressure equation uses a homogeneous Neumann boundary condition at all boundaries, and at the outlet, the mean pressure is set to zero. The convection terms are discretized using a first-order upwind scheme, and the time terms are discretized using a second-order backward scheme. The time step is 2.7 10^{-4}, yielding a maximum Courant number of 5, and a mean Courant number of 0.2.

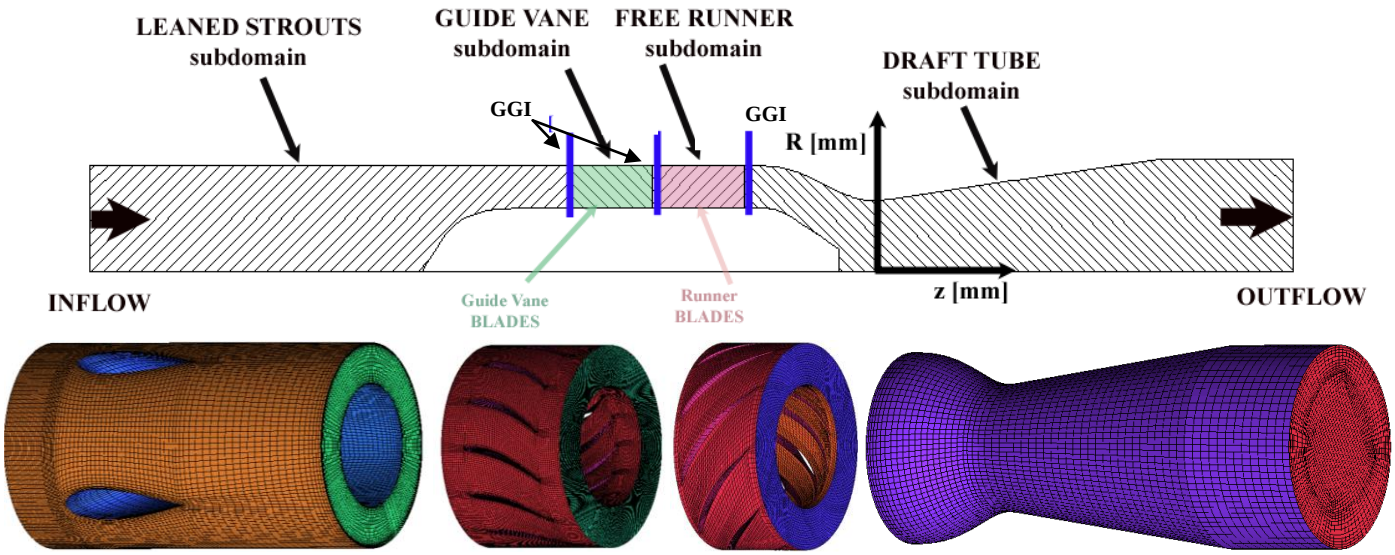

Fig. 4 . Half of meridional cross-section of the swirling flow apparatus (above) and associated computational domains and grids (below).

Two different computational techniques were used to predict the flow in the swirling flow test rig:

- The first method is a steady-state method, solving the steady Reynolds Averaged Navier Stokes equations. Because of the rotor-stator interaction in this case study, a frozen rotor solver is used. It is a steady state formulation where the rotor and stator are fixed with respect to each other, and different reference frames are used in the rotating and stationary parts. Though this method does not predict the flow features behind the runner accurately, it is a fast preliminary method and the general behavior of the flow is predicted.
- The sliding grid approach is a transient method where the runner mesh actually rotates with respect to the stator mesh. The URANS equations are solved and most of the unsteady flow features are predicted. However, due to the extra dimension added to the resolution (time), the simulation is time and computer resources consuming. The interaction between the rotor and stator is realized with the help of a sliding General Grid Interface [13].

However, it was shown in previous studies [14] that the prediction of the flow features by the steady-state method is not accurate enough. So the initial condition of the unsteady simulation is generated by the steady simulation, but the present work is focusing only on the unsteady results, and a comparison of those results with experimental and designed velocity profiles [5] is shown.

4. Comparison of numerical results against experimental and design data

3.1 Designed and computed velocity profiles for swirl generator

The comparison between the designed velocity profiles [5] and OpenFOAM is realized at four Section 1 (S1) and Section 2 (S2) shown in Fig. 5. The dimensionless velocity profiles are plotted against the radius of the different sections, divided by R_{throat}. Section 1 is downstream the guide vanes, and section 2 is downstream the free runner. The results computed by OpenFOAM, are time averaged. The results are shown in Fig. 6 and 7. The two velocity profiles at section 1 and 2 were designed for the swirling flow downstream in the draft tube. At section 1, the swirl created by the guide-vanes should have a free-vortex configuration, with quasi-constant axial velocity. The numerical results obtained with OpenFOAM are in good agreement with the designed profile, see Fig. 6. At section 2, although the axial velocity follows the intended profile rather well, the tangential velocity can not reach the intended value near the shroud, as shown in Fig. 7. This is probably due to the error in the rotational velocity of the runner. The error in prediction for the tangential velocity can be observed at each comparisons section located below the runner. If the velocity of the runner is corrected to the one that gives a free torque, the prediction of the tangential velocity should be more accurate.

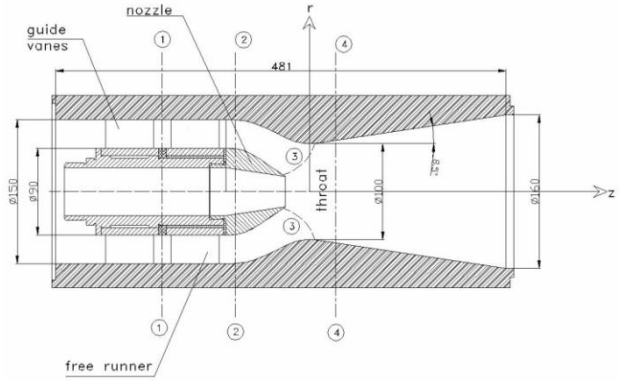

Fig. 5: Cross-section of the swirling flow apparatus and the four survey axes.

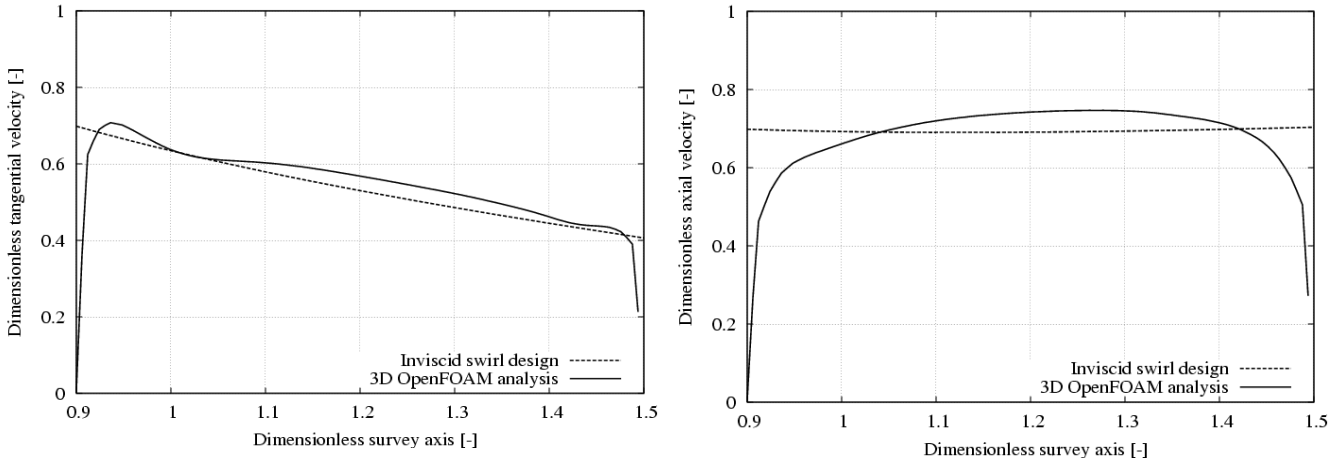

Fig. 6: Tangential and axial velocity profiles at section S1.

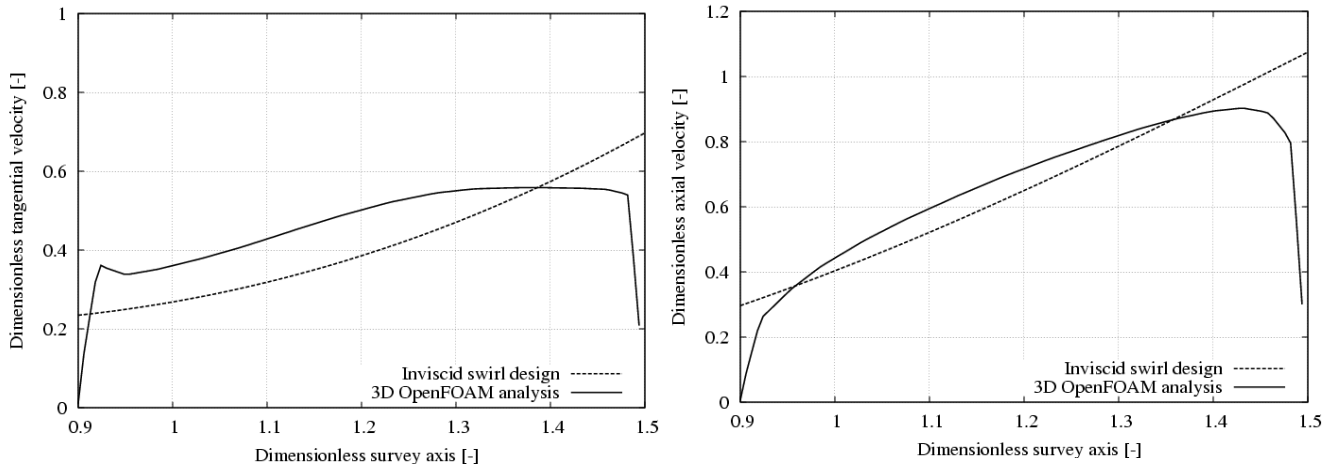

Fig. 7: Tangential and axial velocity profiles at S2.

3.2 Experimental and computed velocity profiles in test the section

The comparisons between the velocity profiles numerically predicted with OpenFOAM and experimental data are shown in Fig. 8. The computed velocity profiles are time averaged over one vortex rope period.

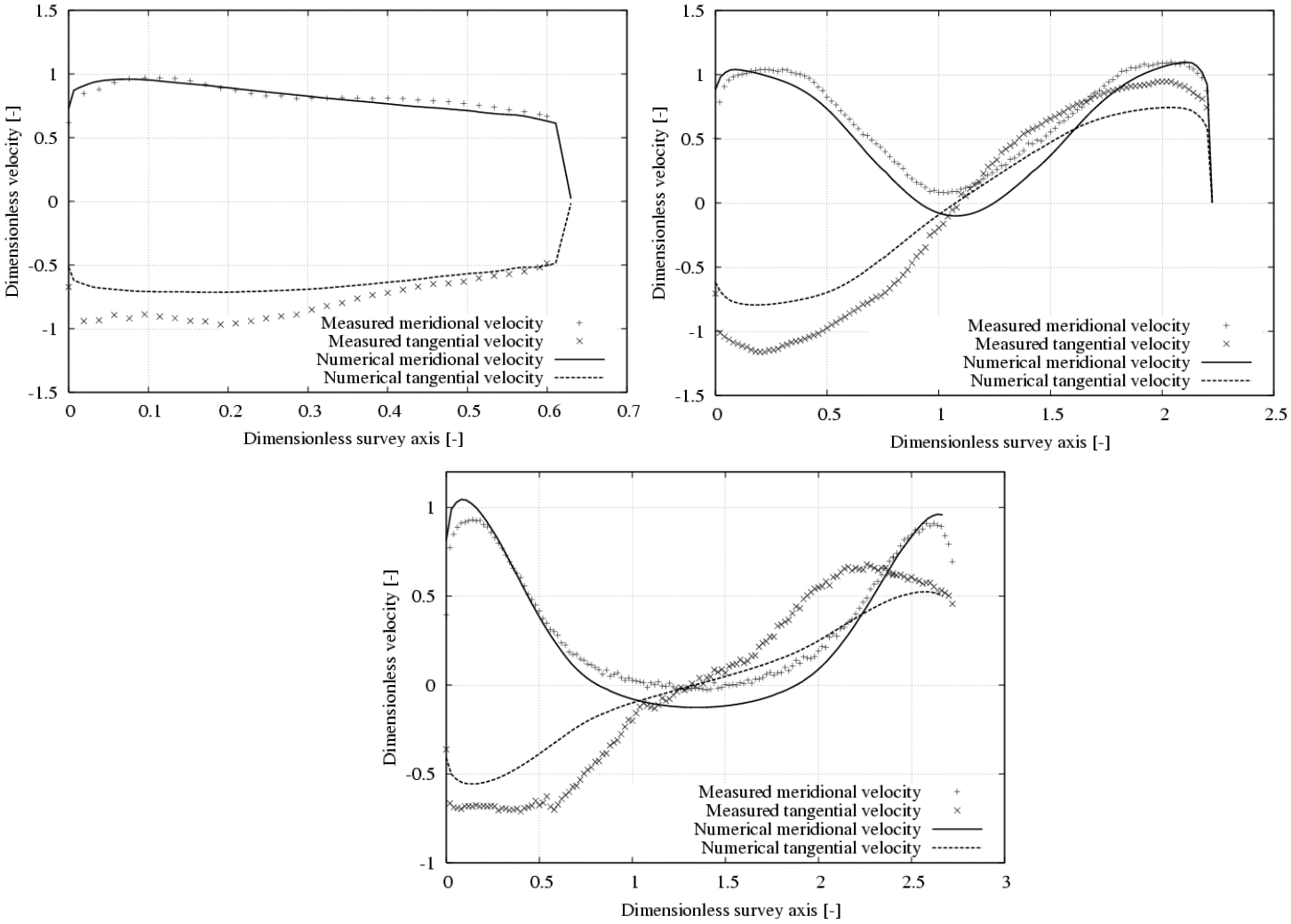

Fig. 8: Velocity profiles at W0 (top left), W1 (top right) and W2 (bottom).

At the first section W0, the numerical meridional velocity computed by OpenFOAM shows very good agreement with that of the experiment**.** However, the computed tangential velocity is a bit under predicted. This could be due to an underestimation of the runner speed. With a higher runner speed, the swirling flow should get stronger. This underestimation of the tangential velocity is

found as well in the comparisons at sections W1 and W2, and has an impact on the stagnation region that can be seen in Fig. 8, at W1 and W2. Since the tangential velocity is not as large as it should be, more flow is pushed close to the walls, and less in the centre line. It can be seen that the stagnation region predicted by the measurements is becoming a recirculation region for the computed flow, with negative meridional velocity. This can probably be avoided by increasing the runner speed.

The slight difference between the numerical results and the measured data can also be justified by the fact that for this simulation, a first-order scheme was set for the convection schemes. A first-order scheme smears out gradients in the flow. A second-order scheme should predict those gradients much better. The unsteady simulation predicts the periodic fluctuations in the draft tube rather well, and a visualization of the computed vortex rope is shown in Fig. 9. Due to the time resolution of the sliding grid model, this visualization of the vortex rope oscillation can be done. Fig. 9 also shows the same vortex rope visualized in the experiments.

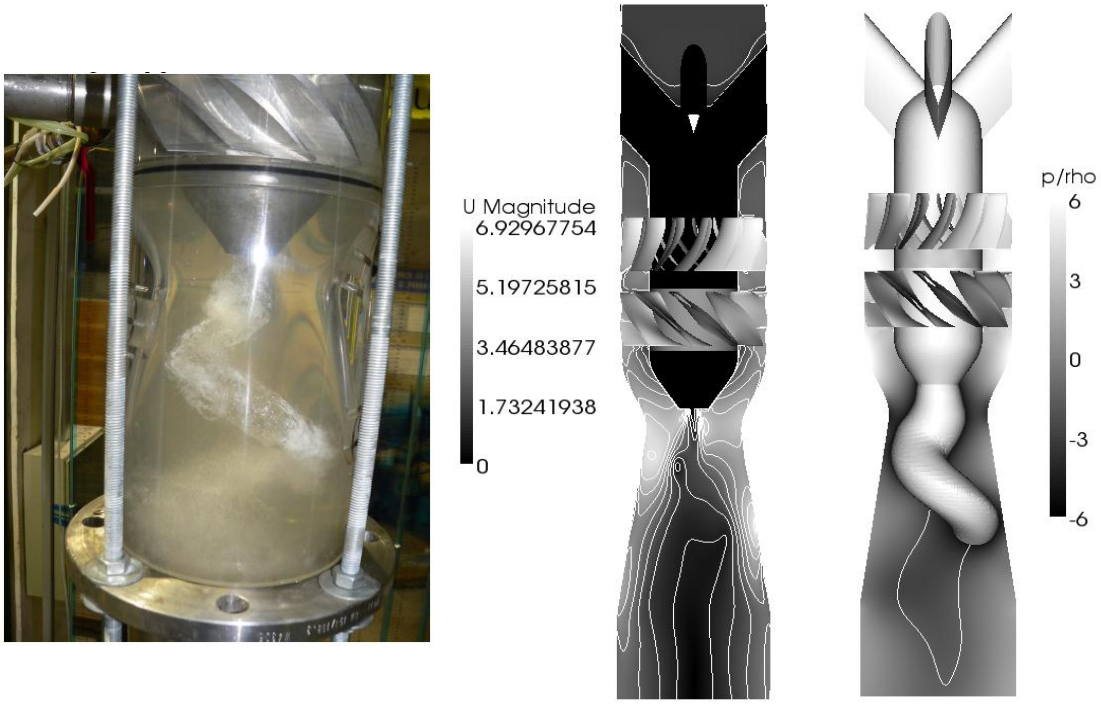

Fig. 9: The precessing vortex rope visualized in the experimental test section (left), and snap-shots of the velocity (centre) and pressure field (right) predicted by the numerical simulations in OpenFOAM. For the pressure snap-shot, the iso-surface visualizes a surface of constant pressure, while the iso-line shows where the axial velocity is zero.

3.3 Free runner speed

In the swirl flow test rig, the runner spins freely, without generating any torque. The measured rotational velocity of the runner while achieving a zero torque is Ω=870 rpm. For such angular velocity, the OpenFOAM simulation gave a negative moment of -0.7 Nm in the axial direction. By linear extrapolation, using a preliminary simulation at Ω=920 rpm, the angular velocity that makes the runner spins freely in OpenFOAM was estimated to be Ω=890 rpm, which was used in the present simulation. On the other hand, the moment reported by the simulation might correspond to the friction in the bearings in the physical model. A study of the impact of the runner speed will be made in the future.

The impact of the vortex rope on the runner moment is shown in Fig. 10, where it is possible to see two main frequencies. The low frequency is due to the rotating vortex rope, creating an oscillation in the runner torque, while the high frequency represents the rotor-stator interaction. This will be analyzed thoroughly in future studies. From Fig. 10, the average value of the moment can be evaluated to about -0.079 Nm. Though it is reasonably close to zero, a more accurate runner velocity can surely be found, and should give slightly higher swirling flow, and thus a better prediction of the tangential velocity and stagnation region.

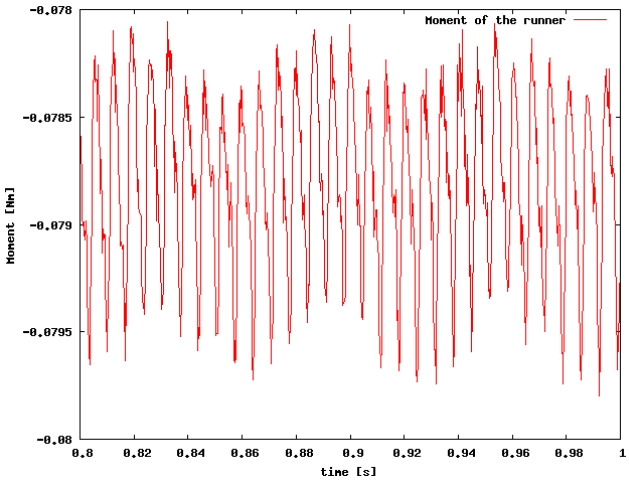

Fig. 10: Torque of the runner as a function of time.

5. Conclusion

Unsteady three-dimensional numerical investigations of the swirling flow with a precessing vortex rope in the swirling flow test rig have been performed. The flow is computed using the standard k-ε model in OpenFOAM. The velocity profiles predicted by the CFD code are accurate, and in good agreement with experimental LDV measurements and designed velocity profiles. The tangential velocity is under estimated, which is probably related to the inaccuracy that comes with the first-order scheme for the convection, and to the value of the runner moment. A more accurate turbulent model than k-ε (such as LES, or DES) should improve the predicted turbulent flow features in the middle of the cone. The same can be said by using a second-order scheme instead of a first-order for the convection terms.

Future work is to find the accurate runner speed for which in OpenFOAM the runner spins freely. An investigation of different turbulence models should as well lead to a better prediction of the flow, and the computed periodic draft tube pressure should be validated with experimental results.

Acknowledgements

Olivier Petit and Prof. Håkan Nilsson are financed by the Swedish Hydropower Centre (SVC). SVC has been established by the Swedish Energy Agency, Elforsk and Svenska Kraftnät together with Luleå University of Technology, The Royal Institute of Technology, Chalmers University of Technology and Uppsala University, www.svc.nu. They would like to would like to thank the Swedish National Infrastructure for Computing (SNIC) and Chalmers Centre for Computational Science and Engineering (C^3SE) for providing computational resources.

A. Bosioc, Dr. Sebastian Muntean and Prof. Romeo Susan-Resiga would like to thank the support of Romanian National Authority for Scientific Research through the CNCSIS PCE 799 project.

References

[1] Avellan, F., 2000, "Flow Investigation in a Francis Draft Tube: The FLINDT Project", in Proceedings of the 20th IAHR Symposium on Hydraulic Machinery and Systems, Charlotte, USA. Paper DES-11.

[2] Susan-Resiga, R., Muntean, S., Bosioc, A., Stuparu, A., Milos, T., Baya, A., Bernad, S., and Anton, L.E., 2007, "Swirling Flow Apparatus and Test Rig for Flow Control in Hydraulic Turbines Discharge Cone", in Proceedings 2nd IAHR International Meetings of the Workgroup in Cavitation and Dynamic Problems in Hydraulic Machinery and Systems, Scientific Bulletin of the Politehnica University of Timisoara, Transcations on Mechanics, Vol. 52(66), Fasc.6, pp. 203-216.

[3] Susan-Resiga, R., Muntean, S., Tanasa, C., and Bosioc, A., 2008, "Hydrodynamic Design and Analysis of a Swirling Flow Generator", in Proceedings of the 4th German – Romanian Workshop on Turbomachinery Hydrodynamics (GRoWTH), June 12-15, 2008, Stuttgart, Germany.

[4] Bosioc, A., Susan-Resiga, R., and Muntean, S., 2008, "Design and Manufacturing of a Convergent-Divergent Test Section for Swirling Flow Apparatus", in Proceedings of the 4th German – Romanian Workshop on Turbomachinery Hydrodynamics (GRoWTH), June 12-15, 2008, Stuttgart, Germany.

[5] Susan-Resiga, R., Muntean, S., and Bosioc, A., 2008, "Blade Design for Swirling Flow Generator", in Proceedings of the 4th German – Romanian Workshop on Turbomachinery Hydrodynamics (GRoWTH), June 12-15, 2008, Stuttgart, Germany.

[6] Susan-Resiga, R., Vu, T.C., Muntean, S., Ciocan, G.D., and Nennemann, B., 2006, "Jet Control of the Draft Tube Vortex Rope in Francis Turbines at Partial Discharge", in Proceedings of the 23rd IAHR Symposium on Hydraulic Machinery and Systems, Yokohama, Japan, Paper F192.

[7] Muntean, S., Susan-Resiga, R., Bosioc, A., Stuparu, A., Baya, A., Anton, L.E., 2008, "Mitigation of Pressure Fluctuation in a Conical Diffuser with Precessing Vortex Rope Using Axial Jet Control Method", in Proceedings of the 24th IAHR Symposium on Hydraulic Machinery and Systems, Foz do Iguassu, Brazil.
[8] Muntean, S., Susan-Resiga, R., and Bosioc, A., 2009, "Numerical Investigation of the Jet Control Method for Swirling Flow with Precessing Vortex Rope", in Proceedings of the 3rd IAHR International Meeting of the Workgroup on Cavitation and Dynamic Problem in Hydraulic Machinery and Systems, Brno, Czech Republic.
[9] Susan-Resiga, R., and Muntean, S., 2008, "Decelerated Swirling Flow Control in the Discharge Cone of Francise Turbines", in Proceedings of the 4th International Symposium on Fluid Machinery and Fluid Engineering, Beijing, China. Paper IL-18.
[10] Bosioc, A., Susan-Resiga, R., and Muntean, S., 2009, "2D LDV Measurements od Swirling Slow in a Simplified Draft Tube", in Proceedings of the CMFF.
[11] Muntean, S., Nilsson, H., and Susan-Resiga, R., 2009, "3D Numerical Analysis of the Unsteady Turbulent Swirling Flow in a Conical Diffuser Using Fluent and OPENFOAM", in Proceedings of the 3rd IAHR International Meeting of the Workgroup on Cavitation and Dynamic Problem in Hydraulic Machinery and Systems, Brno, Czech Republic.
[12] Nilsson, H., Page, M., Beaudoin, M. and Jasak H., 2008, "The OpenFOAM Turbomachinery Working Group, and Conclusions from the Turbomachinery Session of the Third OpenFOAM Workshop", in Proceedings of the 24th IAHR Symposium on Hydraulic Machinery and Systems, Foz do Iguassu, Brazil.
[13] Beaudoin, M., and Jasak, H., 2008, "Development of a Generalized Grid Interface for Turbomachinery simulations with OpendFOAM", in Proceedings of the OpenSource CFD International Conference, Berlin, Germany.
[14] Petit, O., Nillson, H., Page, M. and Beaudoin, M., 2009, "The ERCOFTAC Centrifugal Pump OpenFOAM Case-Study", in Proceedings of the 3rd IAHR International Meeting of the Workgroup on Cavitation and Dynamic Problem in Hydraulic Machinery and Systems, Brno, Czech Republic.
[15] Zangeneh, M, 1991, "A Compressible Three-Dimensional Design Method for Radial and Mixed Flow Turbomachinery Blades", International Journal for Numerical Methods in Fluids, 13, pp. 599-624.